american physiological society

JNP JOURNAL OF NEUROPHYSIOLOGY

J Neurophysiol 126: 743–762, 2021.
First published July 28, 2021; doi:10.1152/jn.00152.2021

RESEARCH ARTICLE

Control of Movement

Similar stretch reflexes and behavioral patterns are expressed by the dominant and nondominant arms during postural control

Philipp Maurus,[1] Isaac Kurtzer,[2] Ryan Antonawich,[2] and Tyler Cluff[1,3]

[1]*Faculty of Kinesiology, University of Calgary, Calgary, Alberta, Canada;* [2]*Department of Biomedical Sciences, New York Institute of Technology College of Osteopathic Medicine, Old Westbury, New York; and* [3]*Hotchkiss Brain Institute, University of Calgary, Calgary, Alberta, Canada*

Abstract

Limb dominance is evident in many daily activities, leading to the prominent idea that each hemisphere of the brain specializes in controlling different aspects of movement. Past studies suggest that the dominant arm is primarily controlled via an internal model of limb dynamics that enables the nervous system to produce efficient movements. In contrast, the nondominant arm may be primarily controlled via impedance mechanisms that rely on the strong modulation of sensory feedback from individual joints to control limb posture. We tested whether such differences are evident in behavioral responses and stretch reflexes following sudden displacement of the arm during posture control. *Experiment 1* applied specific combinations of elbow-shoulder torque perturbations (the same for all participants). Peak joint displacements, return times, end point accuracy, and the directional tuning and amplitude of stretch reflexes in nearly all muscles were not statistically different between the two arms. *Experiment 2* induced specific combinations of joint motion (the same for all participants). Again, peak joint displacements, return times, end point accuracy, and the directional tuning and amplitude of stretch reflexes in nearly all muscles did not differ statistically when countering the imposed loads with each arm. Moderate to strong correlations were found between stretch reflexes and behavioral responses to the perturbations with the two arms across both experiments. Collectively, the results do not support the idea that the dominant arm specializes in exploiting internal models and the nondominant arm in impedance control by increasing reflex gains to counter sudden loads imposed on the arms during posture control.

NEW & NOTEWORTHY A prominent hypothesis is that the nervous system controls the dominant arm through predictive internal models and the nondominant arm through impedance mechanisms. We tested whether stretch reflexes of muscles in the two arms also display such specialization during posture control. Nearly all behavioral responses and stretch reflexes did not differ statistically but were strongly correlated between the arms. The results indicate individual signatures of feedback control that are common for the two arms.

feedback control; handedness; internal model; mechanical perturbations; stretch reflexes

INTRODUCTION

Humans prefer to use one arm over the other when performing motor actions like throwing a ball or eating soup with a spoon. The preference for performing motor actions with one arm is referred to as limb dominance, with the dominance of a particular side being referred to as handedness. About 90% of the human population are right-hand dominant (1) and display preference for performing motor actions with their right arm. Limb dominance may reflect the combined influences of genetic and environmental factors (2), with preferences emerging in gestation (3) that largely predict limb dominance in adolescence (4).

Limb dominance may arise from asymmetries in neural processing across the cerebral hemispheres (5), like those shown for language (6–8). A prominent hypothesis is that limb dominance arises because each hemisphere specializes in different aspects of arm control (9–11). The dominant hemisphere is hypothesized to better leverage an internal model of limb dynamics, capitalizing on biomechanical properties of

Correspondence: P. Maurus (phil.maurus@gmail.com); T. Cluff (tyler.cluff@ucalgary.ca).
Submitted 5 April 2021 / Revised 22 July 2021 / Accepted 23 July 2021

the arm and interactions between segments to produce efficient reaching movements (12). In contrast, the nondominant hemisphere is hypothesized to rely more on impedance control to enable sensitive responses to feedback arising from individual joints (i.e., local feedback) and effective control of static limb postures, as evidenced by more accurate movement end points in the nondominant arm (13). The hypothesis is also supported by asymmetric patterns of sensorimotor adaptation in healthy individuals (14, 15) and after clinical deficits (16–18). Lateralization is further supported by secondary evidence from tendon vibration studies that suggests that proprioceptive function is partially lateralized to the right hemisphere (19). Moreover, past studies have reported better performance when matching the position of the nondominant arm in the absence of visual feedback (20, 21).

Mechanical perturbations are an important probe into how sensory feedback is utilized in motor control (22, 23). The approach of disturbing the arm and measuring muscle responses has revealed that a prevoluntary response, termed the long-latency stretch reflex, incorporates an internal model of the dynamics of the dominant arm (24–30). The internal model for the long-latency reflex (45–105 ms after perturbation) integrates information about the motion of local and remote joints to appropriately counter the underlying torque perturbation. Other evidence suggests that the internal models involved in long-latency reflexes can be adapted when reaching in different environments or with altered properties of the arm (31–35).

After 50+ years of research, all but a few perturbation studies have focused on stretch reflexes in the dominant arm or the coordination between arms. An important exception is a study by Walker and Perreault (36) where the dominant or nondominant elbow was displaced during a posture control task while participants interacted with stable or unstable environments. The task was performed with the dominant and nondominant arms in counterbalanced order. A constant load was used to preexcite motor neuron pools of the elbow muscles in each trial. Servo-controlled displacements were then applied to the elbow joint. Participants were instructed to ignore the perturbations and were not required to return their limb to its initial posture to complete the trial. The authors found that background activity as well as short- and long-latency stretch reflexes of the elbow muscles were amplified in the nondominant arm. Moreover, the stretch reflexes increased in the unstable environment to a similar extent in both arms. The authors argued that participants may have strategically elevated muscle activity in the nondominant arm. Increased background muscle activity would allow the nervous system to amplify stretch reflexes because of the gain-scaling properties of spinal motor neurons (37, 38), thereby creating more vigorous behavioral responses when the nondominant arm is disturbed by the same perturbations during upper limb posture control (39).

The extent to which muscle stretch reflexes differ across the arms, in terms of both the internal model of limb dynamics and overall sensitivity to perturbations, remains unresolved. Detailed examination of the internal model requires investigating how information is integrated across the shoulder and elbow joints while countering perturbations that produce different combinations of joint motion. Here, we imposed loads in different directions to probe the internal model of limb dynamics in the dominant and nondominant arms (24, 25). Task performance was measured by using kinematic outcomes (e.g., return times, peak hand and joint displacements, linearity of hand and joint paths) to characterize behavioral responses when the upper limbs are disturbed by a perturbation (13, 33, 40, 41). Corrective responses were also quantified in terms of the magnitude and directional tuning of stretch reflexes. Together, these measures gauge the nervous system's reliance on an internal model of limb dynamics versus the gain of stretch reflexes. The approach provides an important test of the hypothesis that the nervous system is specialized for impedance control with local modulation of sensory feedback from the nondominant arm and an internal model of limb dynamics that integrates multijoint motion into reflexive responses in the dominant arm (Fig. 1).

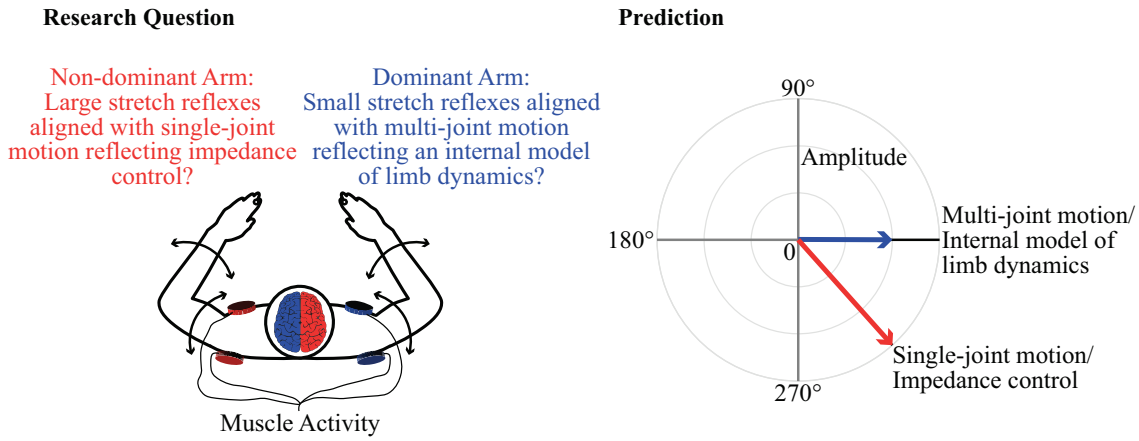

Figure 1. Research question and prediction. Past research has led to the idea that the dominant hemisphere better leverages an internal model of limb dynamics to produce efficient control of the arm (9–11). In contrast, the nondominant hemisphere is thought to rely more on impedance control through sensitive but local modulation of sensory feedback to control the posture of the arm. We examined whether stretch reflexes also display such specialization in upper limb posture control. Specialized reflex function would lead to smaller stretch reflexes that are aligned with multijoint motion in the dominant arm (reflecting an internal model of limb dynamics) and larger stretch reflexes that are aligned with single-joint motion in the nondominant arm (reflecting impedance control). See MATERIALS AND METHODS for further explanation.

MATERIALS AND METHODS

Subjects

Twenty-eight healthy individuals (19–34 yr of age; 16 females, 12 males) participated in one of two experiments. *Experiment 1* was conducted by P. Maurus and T. Cluff. *Experiment 2* was performed by R. Antonawich and I. Kurtzer. The experiments used complementary methods to examine the response magnitude and tuning of stretch reflexes during upper limb postural control (24, 25). The experiments took between 90 and 120 min to complete. All participants were right-handed according to the Edinburgh Handedness Inventory (42), with an average laterality quotient of 86.4% (SE 2.7%). The participants had normal or corrected-to-normal vision and reported no neurological or musculoskeletal impairments. The protocols were approved by the University of Calgary Conjoint Health and Research Ethics Board (*experiment 1*) or the ethics committee at the New York Institute of Technology College of Osteopathic Medicine (*experiment 2*). Participants provided written informed consent before the experiment, were compensated for their time, and were free to withdraw from the study without penalty.

Apparatus

Participants performed the experiments while seated in a robotic exoskeleton (Kinarm, Kingston, ON, Canada). The robot permits upper limb motion in the horizontal plane and can apply independent mechanical loads at the shoulder and/or elbow joints (43, 44). Targets and real-time feedback cursors (white, 0.5-cm radius, aligned with index fingertip) were projected into the plane of motion with an LCD monitor and a semisilvered mirror. A metal barrier blocked direct vision of the upper limbs.

Experiment 1

Thirteen individuals (mean age = 26.3 yr, SE = 1.1 yr; 8 females, 5 males) countered mechanical perturbations while attempting to maintain a fixed arm posture (24). At the beginning of each trial, the LCD monitor displayed a start target (0.5-cm radius) surrounded by a larger, concentric return target (2-cm radius). The start target maintained the same elbow and shoulder angle across participants and arms. The shoulder angle was 45° relative to the frontal plane, and the elbow angle was 75° relative to the upper arm (0° indicating full extension; Fig. 2*A*). Subjects began each trial by moving their hand feedback cursor into the start target. After a brief delay (2,000 ± 1,500 ms, uniformly distributed), step torque perturbations (±2 Nm, 10-ms sigmoidal ramp-to-constant profile) were applied at the shoulder and/or elbow joints (24). We used six perturbations with different combinations of shoulder and elbow torques (Fig. 2*B*). Background loads were not applied in this experiment. The hand feedback cursor was removed at the onset of the perturbation to ensure that corrective responses were based on proprioceptive feedback (14, 24). Participants were instructed to return to the target within 500 ms and briefly hold this position (1,000 ms). The circle turned green if participants returned to the target within the time limit and held this position and blue if they were inaccurate or too slow. The load then slowly ramped down (1,000-ms sigmoidal ramp-to-constant profile) and remained off for 1,000 ms before the next trial. Trials were performed one arm at a time, and the order of trials was block-randomized across arms. Each block contained 12

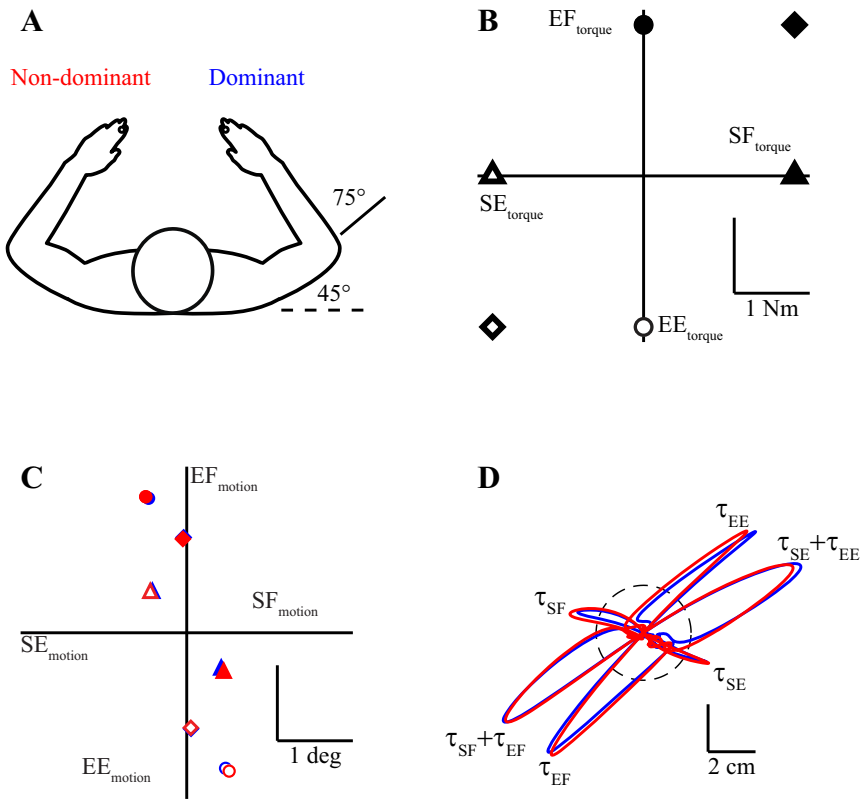

Figure 2. Experimental setup and perturbation-evoked displacements in *experiment 1*. *A*: initial limb configuration in *experiment 1*. *B*: applied torques in *experiment 1*. We applied shoulder flexion (SF), shoulder extension (SE), elbow flexion (EF), elbow extension (EE), and combined torques. *C*: group average evoked joint motion at 50 ms after perturbation onset. Symbols are aligned to the torque perturbations presented in *B*. The nondominant arm was displaced farther than the dominant arm in the single-joint shoulder perturbation conditions. *D*: group average hand paths for *experiment 1*. Note that the data for the left arm have been reflected about the vertical axis. Dashed black circle indicates the outer boundary of the target; τ indicates the perturbation condition.

trials presented in random order (2 arms × 6 perturbations). Participants performed 40 trials for each torque combination, resulting in a total of 480 trials.

Experiment 2

Fifteen individuals (mean age = 24.9 yr, SE = 0.4 yr; 8 females, 7 males) performed a postural control task while countering perturbations that were designed to generate near-uniform patterns of joint motion (25). We first determined the torques required to evoke near-uniform joint displacements for each subject. The procedure involved applying eight torque pulse perturbations spaced evenly in joint-torque space. Perturbations were repeated five times in block-randomized order, where each block contained one of each type of perturbation. The perturbations were applied one hand at a time, resulting in a total of 40 trials/arm (8 perturbations × 5 trials). Participants completed this procedure with their dominant or nondominant arm in counterbalanced order. We then estimated the torques required to displace each participant's arm by a fixed amount (resultant displacement of 1° in 50 ms) in eight near-uniformly-spaced directions in joint space (25).

In the main experiment, individuals stabilized their hand-aligned cursor within a start target (2.5-cm radius) positioned at a shoulder angle of 60° and an elbow angle of 75° (0° is full extension; see Fig. 9*A*). The robotic device then applied constant background loads to preexcite the brachioradialis and posterior deltoid muscles (1.5 Nm, 500-ms ramp-to-constant profile). Hand cursor feedback was extinguished while participants held their hand in the start target against the background loads. After a random time interval (2,250 ± 1,250 ms, uniformly distributed), we disturbed the participant's arm with a torque pulse perturbation (80 ms with 10-ms linear ramp-to-constant profile). Subjects were required to return to the target within 500 ms and hold this position for 500 ms. The circle turned green if participants returned to the target within the time limit and held this position and red if they were inaccurate or too slow. The background loads were turned off (1,000-ms ramp-down time) and remained off between trials (2,500 ms). Participants performed a total of 480 trials (8 perturbations × 30 trials × 2 arms). Again, participants completed the task with their dominant and nondominant arms. The task was performed one arm at a time. Half of the participants performed the task with their dominant arm first, and the other half started with their nondominant arm.

Data Analysis

Kinematic recordings and analysis.

Kinematic data were sampled at 1 kHz. The data were low-pass filtered (2nd-order, dual-pass Butterworth filter, 30-Hz cutoff) before further analysis (33, 45). We calculated each participant's average hand and joint motion profiles for each torque combination and arm. Shoulder and elbow displacement were determined 50 ms after perturbation onset for each trial and arm (24, 25). Motor behavior was characterized by calculating the peak hand displacements, peak joint displacements, return times, end point accuracy, linearity of hand paths, and linearity of joint paths in individual trials. Note that all kinematic parameters were calculated based on hand position, which was defined as the center of the hand feedback cursor. Return times were calculated as the time between when the participant's hand left and returned to the target (41, 45, 46). End point accuracy was determined as the distance between the center of the goal target and hand position when the hand speed reached the first local minimum below a threshold of 5 cm/s (40, 41). We assessed the linearity of hand paths by extracting the maximum distance perpendicular to the peak displacement and dividing it by

Table 1. *Outcomes of the two-way repeated-measures ANOVAs for motor behavior in experiment 1*

Outcome Measure	Effect	*F* Statistics	*P* Value	η^2
Elbow angle at 50 ms	Hand	$F(1,12) = 0.98$	0.342	0.001
	Perturbation	$F(1.02,12.28) = 507.19$	2.13e−11	0.976
	Interaction	$F(1.71,20.51) = 8.31$	0.003	0.012
Shoulder angle at 50 ms	Hand	$F(1,12) = 0.75$	0.404	0.001
	Perturbation	$F(1.05,12.65) = 792.83$	6.87e−13	0.984
	Interaction	$F(5,60) = 29.84$	4.31e−15	0.154
Peak hand displacement	Hand	$F(1,12) = 0.02$	0.879	0.000
	Perturbation	$F(1.39,16.67) = 157.27$	1.06e−10	0.725
	Interaction	$F(5,60) = 2.35$	0.051	0.008
Peak joint displacement	Hand	$F(1,12) = 0.49$	0.496	0.002
	Perturbation	$F(1.67,20.02) = 135.27$	7.64e−12	0.628
	Interaction	$F(2.32,27.86) = 2.04$	0.143	0.007
Return time	Hand	$F(1,12) = 0.17$	0.690	0.000
	Perturbation	$F(3.03,36.41) = 10.51$	3.82e−05	0.170
	Interaction	$F(5,60) = 1.47$	0.213	0.016
End point accuracy	Hand	$F(1,12) = 0.04$	0.842	0.000
	Perturbation	$F(2.03,24.38) = 37.78$	3.08e−08	0.582
	Interaction	$F(5,60) = 0.25$	0.940	0.003
Linearity of hand paths	**Hand**	$F(1,12) = 15.05$	0.002	0.024
	Perturbation	$F(2.18,26.21) = 15.14$	2.88e−05	0.350
	Interaction	$F(5,60) = 0.49$	0.784	0.005
Linearity of joint paths	**Hand**	$F(1,12) = 20.02$	7.61e−04	0.017
	Perturbation	$F(2.25,27.03) = 80.09$	1.60e−12	0.753
	Interaction	$F(5,60) = 2.49$	0.040	0.025

Statistically significant effects are presented in bold.

the peak displacement (14). Hand path linearity has been used to infer the nervous system's use of an internal model of limb dynamics (47). The applied perturbations in our experiments consisted of different combinations of step torques applied to the joints and often evoked curved hand trajectories. Thus, we also investigated the linearity of joint paths by determining the maximum joint distance perpendicular to the peak joint displacement and dividing it by the peak joint displacement. The kinematic measures were averaged separately for each participant's left and right arms. If the control of reflex responses is specialized and asymmetric across the arms (9–11), smaller peak hand displacements, shorter return times, and higher end point accuracy would be expected in the nondominant arm. In contrast, greater linearity would be expected in the hand and joint paths of the dominant arm (9–11).

Muscle activity recordings and analysis.

We recorded from monoarticular elbow (brachioradialis, elbow flexor; triceps lateralis, elbow extensor) and shoulder (pectoralis major, shoulder flexor; posterior deltoid, shoulder extensor) muscles in both arms with bipolar surface electrodes (DE 2.1 Single Differential Electrode; Delsys) in *experiment 1*. In *experiment 2*, we recorded the activity of the brachioradialis and posterior deltoid muscles. The muscle activity signals were amplified online (gain = 10^3–10^4) and

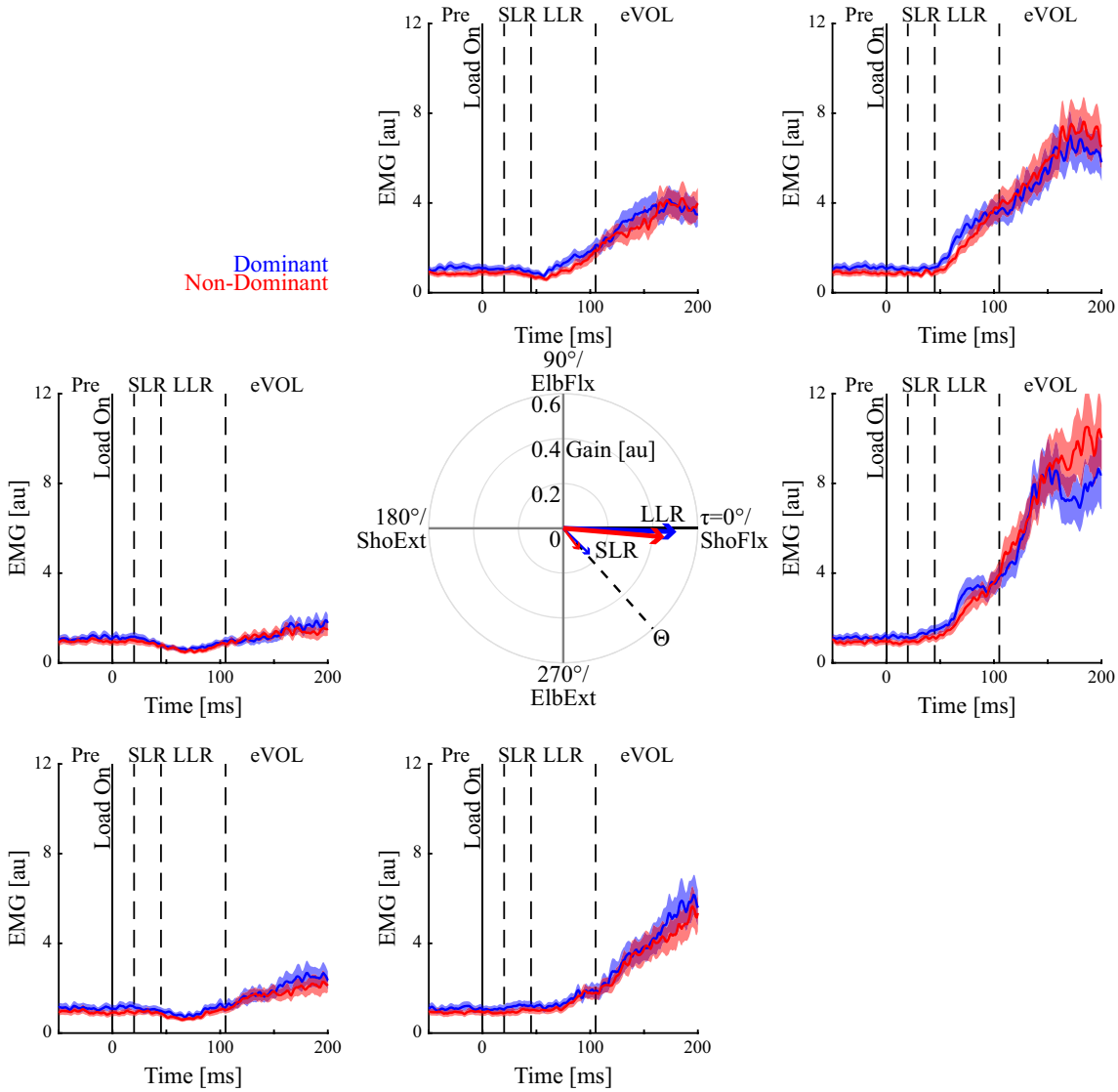

Figure 3. Posterior deltoid muscle activity, preferred torque direction (PTD), and response magnitude in *experiment 1*. Outside panels represent muscle stretch reflexes for each applied torque and are oriented as in Fig. 2*B*. Colored lines indicate group averages of the dominant (blue) and nondominant (red) arms. Shaded areas indicate ±1 SE. Solid vertical lines indicate perturbation onset. Vertical lines separate phases of the stretch reflex: preperturbation activity (Pre: −50 to 0 ms), short-latency reflex (SLR: 20 to 45 ms), long-latency reflex (LLR: 45 to 105 ms), and early voluntary response (eVOL: 105 to 200 ms). *Center*: a polar plot of the average PTDs and response magnitude of posterior deltoid muscle stretch reflexes. The thin arrows reflect the PTD and response magnitude during the SLR. Note that the response magnitude during the SLR was amplified by 2 for visualization purposes. The thick arrows indicate the PTD and response magnitude during the LLR. The dashed black line corresponds to the local PTD (Θ). The solid black line corresponds to the ideal PTD (τ). au, Arbitrary units; ElbExt, elbow extension; ElbFlx, elbow flexion; EMG, electromyogram; ShoExt, shoulder extension; ShoFlx, shoulder flexion.

sampled at 1 kHz. The skin was prepared by cleaning it with alcohol swabs and removing hair if necessary. A ground electrode was placed over the lateral epicondyle of the right elbow.

Muscle activity data were band-pass filtered (3rd-order, dual-pass Butterworth filter, 20 and 450 Hz) and full-wave rectified (24, 48). In *experiment 1*, the activity of brachioradialis, triceps lateralis, pectoralis major, or posterior deltoid muscles was normalized to the average activity required to counter 1-Nm reference loads that excited the corresponding muscle while holding the start position (33, 45, 49). The normalization task was performed after the main experiment and consisted of five 15-s trials for each load direction (elbow extension, elbow flexion, shoulder extension, shoulder flexion loads). The first 3 s after load onset of each trial was discarded to avoid transient responses in muscle activity. In *experiment 2*, each muscle's activity was normalized to its average activity when countering the background loads (−100 to 0 ms relative to perturbation onset) in each trial (25). The muscle activity data were aligned to perturbation onset. The average muscle activity was calculated during predetermined time windows: −50 to 0 ms [preperturbation activity (Pre)], 20 to 45 ms [short-latency reflex (SLR)], 45 to 105 ms [long-latency reflex (LLR)], and 105 to 200 ms [early voluntary response (eVOL)]. We averaged each participant's muscle activity within each time window in individual trials (33). Past research proposed that the nervous system specializes in using impedance mechanisms to control the static posture of the nondominant arm (10, 11). We compared the preperturbation activity of each muscle based on the global average across all perturbations. If the nondominant arm relied on greater impedance mechanisms, we expected that preperturbation activity would be elevated compared with the dominant arm (36).

Preferred torque direction, preferred motion direction, and response magnitude.

Because of the inherent intersegmental dynamics of the upper limbs, motion at one joint (e.g., elbow) causes an interaction torque that can displace other joints (e.g., shoulder) (50–52). If the nervous system possesses an internal model of limb dynamics, stretch reflexes should incorporate feedback about motion at both the shoulder and the elbow into a response that is appropriate for their mechanical interactions and the underlying torque perturbation. If the nervous system does not possess an internal model of limb dynamics, stretch reflexes should reflect local/single joint motion. Several studies have shown that stretch reflexes in the SLR time window reflect local muscle stretch, whereas stretch reflexes in the LLR time window account for the motion at other joints and thus possess an internal model of limb dynamics (24–30).

Planar regressions were performed to calculate the preferred torque direction (PTD) of shoulder muscles and assess the extent to which stretch reflexes reflect an internal model of limb dynamics (24). We performed separate planar regressions in the SLR, LLR, and eVOL time windows in *experiment 1* as follows (24):

$$\text{evoked activity} = a(\text{shoulder torque}) + b(\text{elbow torque}) + \text{constant}$$

$$\text{PTD} = \text{atan}\left(\frac{a}{b}\right)$$

In each time window, the PTD was evaluated against two contrasting predictions that examine the sensitivity to shoulder motion versus the underlying shoulder torque. The ideal PTD (τ) for pure shoulder torque is directed at 0/360° for a shoulder flexion torque or 180° for a shoulder extension torque. The predicted local PTD (Θ) for pure shoulder motion is determined by a planar regression of shoulder motion at 50 ms after perturbation against the applied shoulder and elbow torques (24, 27). The calculated local PTDs (Θ's) are 312° (SD 0.5°) for pure shoulder flexion and 132° (SD 0.5°) for pure shoulder extension (24, 27). If the evoked shoulder muscle activity reflects local muscle stretch, the PTDs will be close to Θ. In contrast, the PTDs will be close to τ if the evoked muscle activity reflects an internal model of limb dynamics. A prominent idea is that the nervous system leverages an internal model of limb dynamics to control the dominant arm (9–11). Thus, we examined whether the PTDs of the dominant arm leverage an internal model of limb dynamics (PTDs closer to τ) while the PTDs of the nondominant arm reflect single-joint motion (PTDs closer to Θ). Based on past research, we expected that any

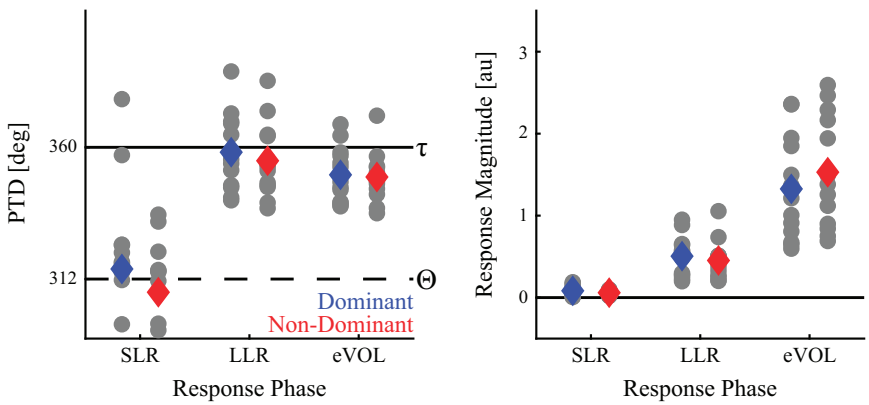

Figure 4. Preferred torque direction (PTD) and response magnitude of posterior deltoid stretch reflexes in *experiment 1*. Colored diamonds depict the group average PTDs and response magnitude of the dominant (blue) and nondominant (red) shoulder extensors across the short-latency reflex (SLR), long-latency reflex (LLR), and early voluntary response (eVOL) time windows. Gray dots represent individual subject data. Dashed black line corresponds to the local PTD (Θ). Solid black line corresponds to the ideal PTD (τ). au, Arbitrary units.

difference in PTDs would be evident in the LLR and eVOL time windows (24–28, 30). In *experiment 1*, PTDs were analyzed for the monoarticular shoulder muscles only (24, 27). This experiment is not designed to assess the PTD of elbow muscles since specific torque combinations, tailored to the inertia of each individual's limbs, are required as used in *experiment 2* (25).

In *experiment 2*, the preferred motion direction (PMD) was determined for the posterior deltoid and brachioradialis muscles. The PMDs are analogous to the PTDs in *experiment 1* and assess whether stretch reflexes reflect an internal model of limb dynamics. The PMDs were determined by performing planar regressions between the evoked muscle activity and motion at the shoulder and elbow joints as follows (25):

$$\text{evoked activity} = a(\text{shoulder angle @ 50 ms}) + b(\text{elbow angle @ 50 ms}) + \text{constant}$$

$$\text{PMD} = \operatorname{atan}\left(\frac{a}{b}\right)$$

PMDs were calculated for the SLR and LLR time windows since the brief torque pulses (80 ms) produced small amounts of joint motion and thus small and variable muscle stretch responses in the eVOL time window (53). Past work

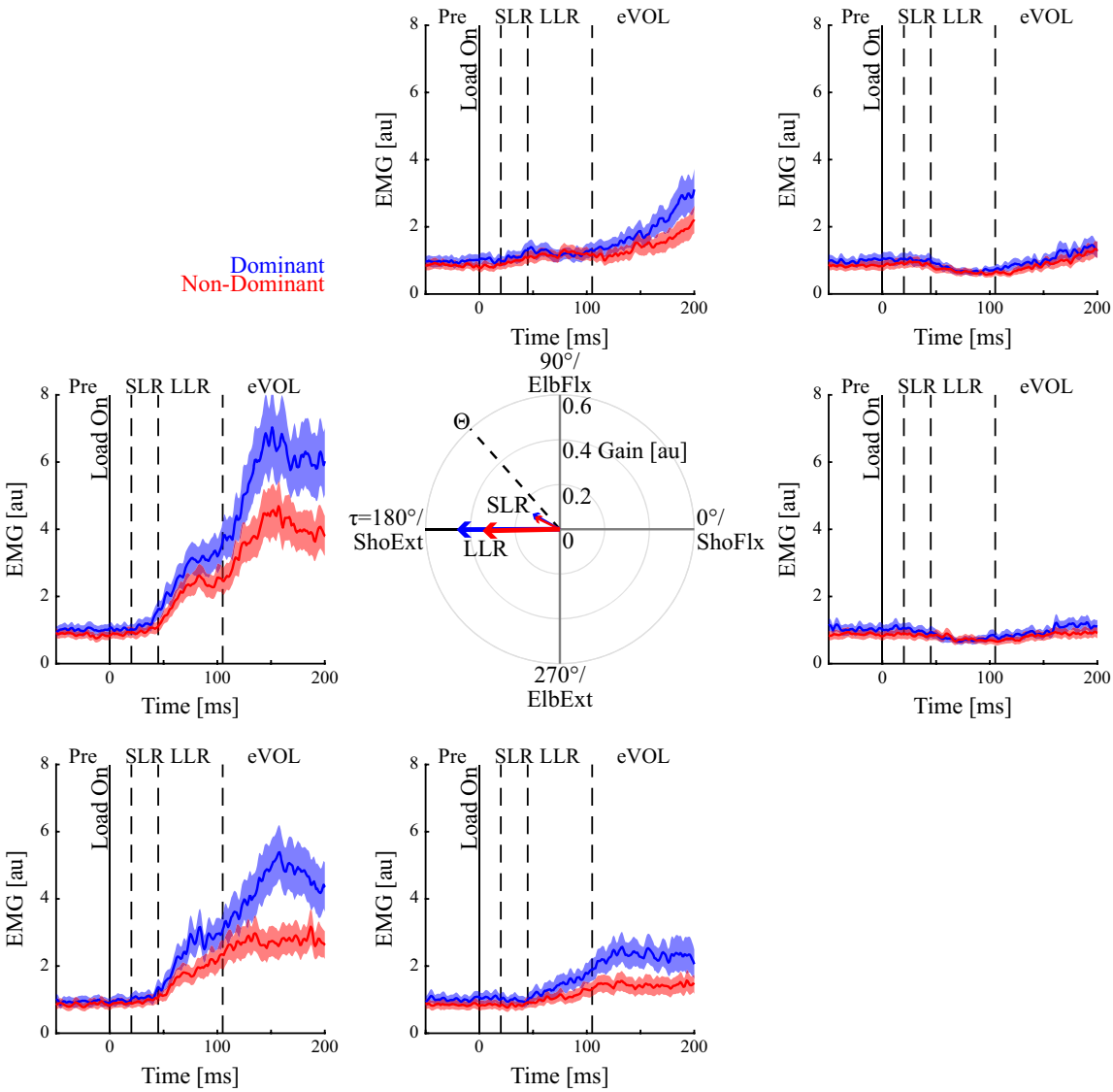

Figure 5. Pectoralis major muscle activity, preferred torque direction (PTD), and response magnitude in *experiment 1*. Outside panels display muscle stretch reflexes for each applied torque and are oriented as in Fig. 2*B*. Colored lines indicate group averages of the dominant (blue) and nondominant (red) arms. Shaded areas indicate ±1 SE. Solid vertical lines indicate perturbation onset. Dashed vertical lines separate phases of the stretch reflex: preperturbation activity (Pre: −50 to 0 ms), short-latency reflex (SLR: 20 to 45 ms), long-latency reflex (LLR: 45 to 105 ms), and early voluntary response (eVOL: 105 to 200 ms). *Center*: a polar plot of the average PTDs and response magnitude of pectoralis major muscle stretch reflexes. The thin arrows reflect the PTD and response magnitude during the SLR. Note that the response magnitude during the SLR was amplified by 2 for visualization purposes. The thick arrows indicate the PTD and response magnitude during the LLR. The dashed black line corresponds to the local PTD (Θ). The solid black line corresponds to the ideal PTD (τ). au, Arbitrary units; ElbExt, elbow extension; ElbFlx, elbow flexion; EMG, electromyogram; ShoExt, shoulder extension; ShoFlx, shoulder flexion.

has reported a ~35% reduction in muscle stretch responses within ~30 ms after the offset of torque perturbations of amplitude similar to those used in the present experiment (53). As a result, muscle activity in the eVOL time window was variable and insufficient for calculating the PMDs.

The cardinal axes in this paradigm correspond to the local PMD (Θ), such that 0/360° is pure shoulder flexion, 180° is shoulder extension, 90° represents elbow flexion, and 270° represents elbow extension. The PMDs in the SLR and LLR time windows will align with the local PMD (Θ) if they are only sensitive to local joint motion. In contrast, the PMDs in the SLR and LLR time windows will align with the ideal PMD (τ) if the responses incorporate an internal model of limb dynamics. The ideal PMDs were 18° (SD 1°) for the posterior deltoid muscle and 225° (SD 2°) for the brachioradialis muscle (25). Akin to *experiment 1*, we asked whether the PMDs of muscles in the nondominant arm are closer to Θ (local joint motion) while the PMDs of muscles in the dominant arm are closer to τ (reflect an internal model of limb dynamics). This effect should be evident in the LLR time window (24–28, 30).

We analyzed the response magnitude of stretch reflexes in the SLR, LLR, and eVOL time windows in *experiment 1* (24). Response magnitudes were determined for the SLR and LLR time windows in *experiment 2* (25) because of the nature of the torque pulse perturbations. The following formula was used to calculate the response magnitude (25):

$$\text{response magnitude} = \sqrt{a^2 + b^2}$$

The response magnitude measures the overall sensitivity or gain of a muscle's reflexive responses to stretch arising from different combinations of applied torques and complements information provided by the PTDs and PMDs (26). There is evidence that the nervous system relies on impedance mechanisms to control the posture of the nondominant arm (9–11). Thus, we examined whether stretch reflexes display larger response magnitudes in nondominant arm muscles. Note that coactivation of muscles in the nondominant arm may lead to upregulation of short- and long-latency reflexes because of automatic gain scaling arising from excitation of spinal motor neurons, particularly if the two arms are displaced similarly (37–39, 54, 55). Alternatively, stretch reflexes of muscles in the nondominant arm could be larger because of a greater sensitivity to stretch in the absence of differences in background muscle activity.

Statistical Analysis

In *experiments 1 and 2*, we compared the motion of the elbow and shoulder joints at 50 ms after perturbation onset, peak hand displacements, peak joint displacements, return times, end point accuracy, and linearity of hand and joint paths between the two arms with a two-way repeated-measures ANOVA (main effect of arm, main effect of perturbation, and interaction effect). In *experiment 2*, we compared the applied elbow and shoulder torques across arms with two-way repeated-measures ANOVAs. The Greenhouse–Geisser correction was used if the data violated the sphericity assumption (Mauchly's test, $P < 0.05$). Where the interaction effect was statistically significant, the repeated-measures ANOVA was decomposed with two-sided, paired *t* tests. All *P* values were adjusted with Bonferroni corrections based on the number of applied perturbations in each experiment (*experiment 1*: 6; *experiment 2*: 8). If there was a statistically significant main effect of arm, the repeated-measures ANOVA was decomposed with planned comparisons. Two-sided, paired *t* tests were used to compare preperturbation muscle activity, PTDs, PMDs, and response magnitudes across the arms. The *P* values for *t* tests within each time window were adjusted with Bonferroni corrections depending on the number of muscles recorded in each experiment (*experiment 1*: 4; *experiment 2*: 2). Effect sizes were determined for the repeated-measures ANOVA with partial η^2 and paired *t* tests using Cohen's *d* (56). We used two-tailed tests because of the limited number of studies comparing reflexive responses to mechanical disturbances across the arms. The threshold for all statistical tests was set to $\alpha = 0.05$. The statistical analyses were performed in RStudio (1.1.463; RStudio Inc.) with the 'tidyverse' and 'rstatix' packages.

The data from *experiments 1* and *2* were combined to investigate the relationship between behavioral measures across the arms. Similarly, we examined the PTDs/PMDs and response magnitude for the posterior deltoid muscle as well as the response magnitude for the brachioradialis muscle during the LLR time window. We averaged motor behavior (e.g., peak hand displacements, peak joint displacements,

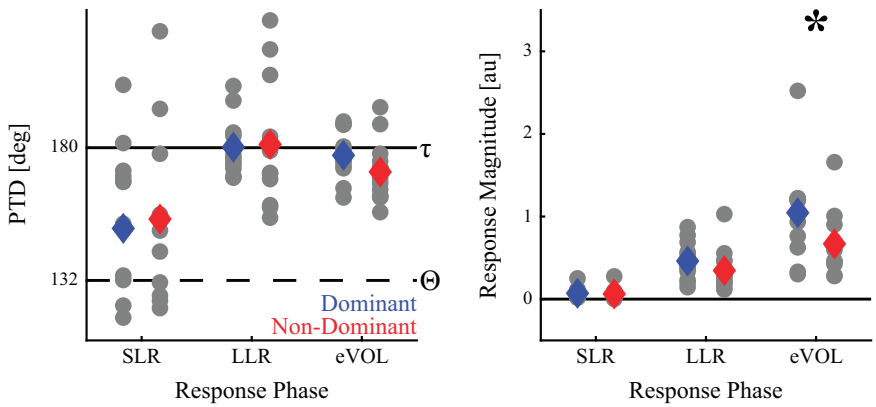

Figure 6. Preferred torque direction (PTD) and response magnitude of pectoralis major stretch reflexes in *experiment 1*. Colored diamonds depict the group average PTDs and response magnitude of the dominant (blue) and nondominant (red) shoulder flexors across the short-latency reflex (SLR), long-latency reflex (LLR), and early voluntary response (eVOL) time windows. Gray dots represent individual subject averages. Dashed black line corresponds to the local PTD (Θ). Solid black line corresponds to the ideal PTD (τ). au, Arbitrary units. *$P < 0.05$.

return times, end point accuracy, linearity of hand paths, and linearity of joint paths) across all perturbations for each individual, arm, and experiment. The kinematic measures, PTDs/PMDs, and response magnitudes were standardized (i.e., *z* transform) within each experiment (30, 51) and subsequently pooled for correlation analysis. Correlation analyses were based on Pearson's product moment correlation coefficient (*r*) and performed in MATLAB (R2020b; MathWorks).

RESULTS

Experiment 1: Arm Kinematics and Motor Behavior

Group average joint kinematics are displayed in Fig. 2*C*. The repeated-measures ANOVA revealed statistical differences in the evoked motion of the dominant and nondominant arms as early as 50 ms after perturbation (Table 1). Post hoc comparisons revealed statistically larger displacements of the nondominant elbow joint (12.2–14.3% or 0.055–0.065°; $P < 0.002$, $d = -1.75$ to -1.38) in two of six perturbation conditions (single-joint shoulder torque perturbations), whereas no statistical differences were found in the remaining four conditions ($P = 0.186$–1.000, $d = -0.68$ to 0.35). The displacements of the nondominant shoulder joints were statistically larger in all single-joint perturbation conditions (4 of 6 directions; 10.7–12.7% or 0.043–0.062°; $P < 0.001$, $d = -1.47$ to -1.69) but not in the multijoint perturbation conditions (2 of 6 directions; $P = 1.000$, $d = -0.09$ to -0.06).

Group average hand paths are shown in Fig. 2*D*. The repeated-measures ANOVAs did not reveal statistical

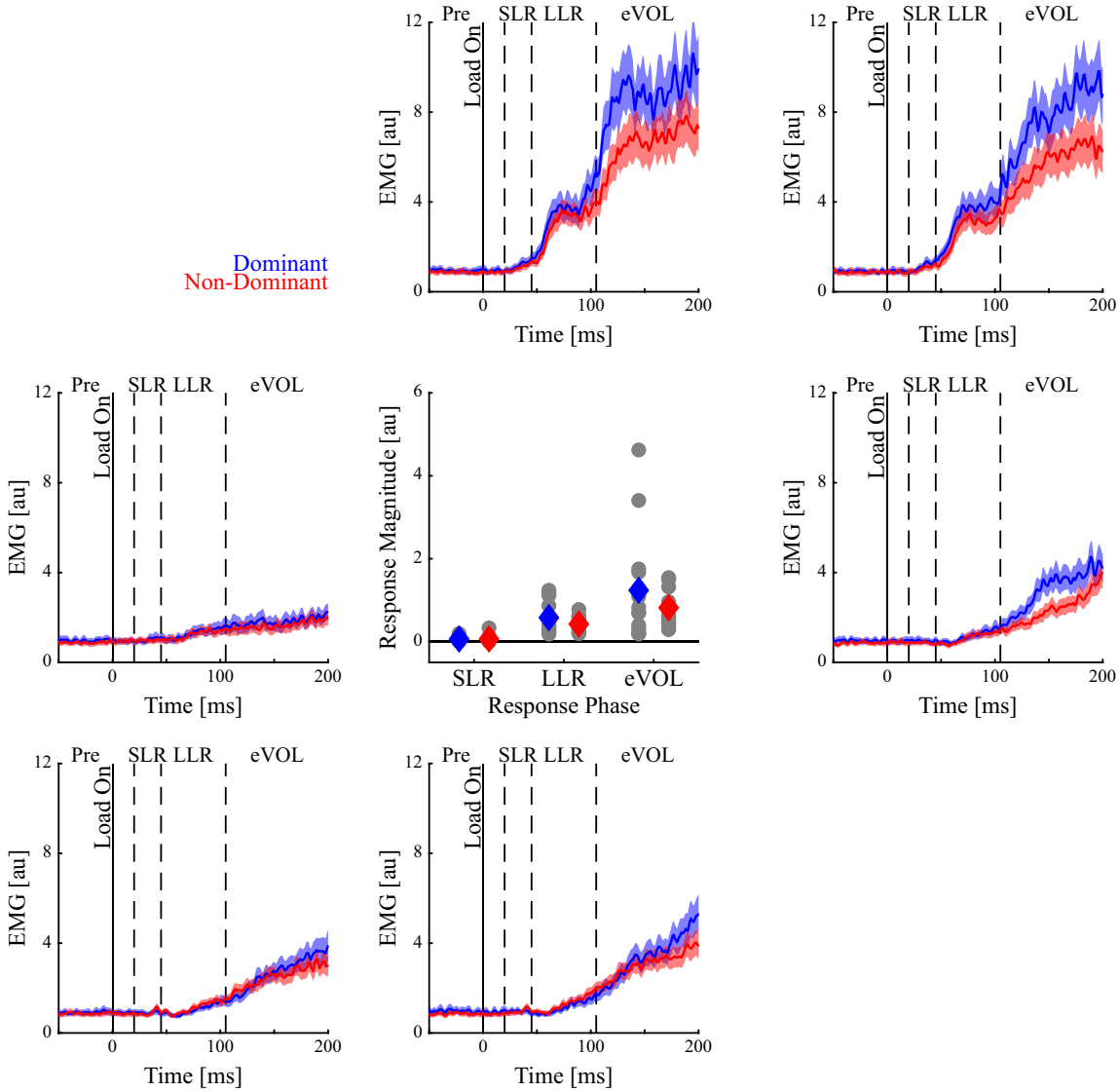

Figure 7. Triceps lateralis muscle activity and response magnitude in *experiment 1*. Outside panels represent muscle stretch reflexes for each applied torque and are oriented as in Fig. 2*B*. Colored lines indicate group averages of the dominant (blue) and nondominant (red) arms. Shaded areas indicate ±1 SE. Solid vertical lines indicate perturbation onset. Vertical lines separate phases of the stretch reflex: preperturbation activity (Pre: −50 to 0 ms), short-latency reflex (SLR: 20 to 45 ms), long-latency reflex (LLR: 45 to 105 ms), and early voluntary response (eVOL: 105 to 200 ms). *Center*: the response magnitude. Colored diamonds depict the group average response magnitude across the SLR, LLR, and eVOL time windows. Gray dots represent individual subject data. au, Arbitrary units, EMG, electromyogram.

differences in peak hand displacements, peak joint displacements, return times, or end point accuracy between the two arms. When comparing the linearity of hand paths between the two arms, we found a statistically significant effect of hand (Table 1). The hand paths of the dominant arm were more linear than the hand paths of the nondominant arm (P = 0.001, d = −1.08). Linearity analyses were also performed on the trajectories of the shoulder and elbow joints, revealing a statistically significant interaction between hand and perturbation direction (Table 1). Joint trajectories were more linear in the dominant arm after the multijoint elbow flexion perturbations (P = 0.018, d = −1.05). Statistical differences were not observed in the remaining five perturbation conditions (P = 0.156–1.000, d = −0.71 to 0.11).

Experiment 1: Preperturbation Activity, Preferred Torque Directions, and Response Magnitude

Next, we investigated the stretch reflexes of the shoulder muscles. We examined the preperturbation activity as well as the PTDs and response magnitude across the different phases of the stretch reflex (Fig. 3 and Fig. 4). The preperturbation activity was not statistically different between the dominant and nondominant posterior deltoid muscles [$t(12)$ = 2.42, P = 0.130, d = 0.67]. The PTDs of the shoulder muscles were examined to determine whether stretch reflexes incorporate only local joint motion (PTDs closer to Θ) or reflect an internal model of limb dynamics (PTDs closer to τ). In alignment with previous findings (24, 25, 27), the PTDs of the posterior deltoid reflected local joint motion during the SLR

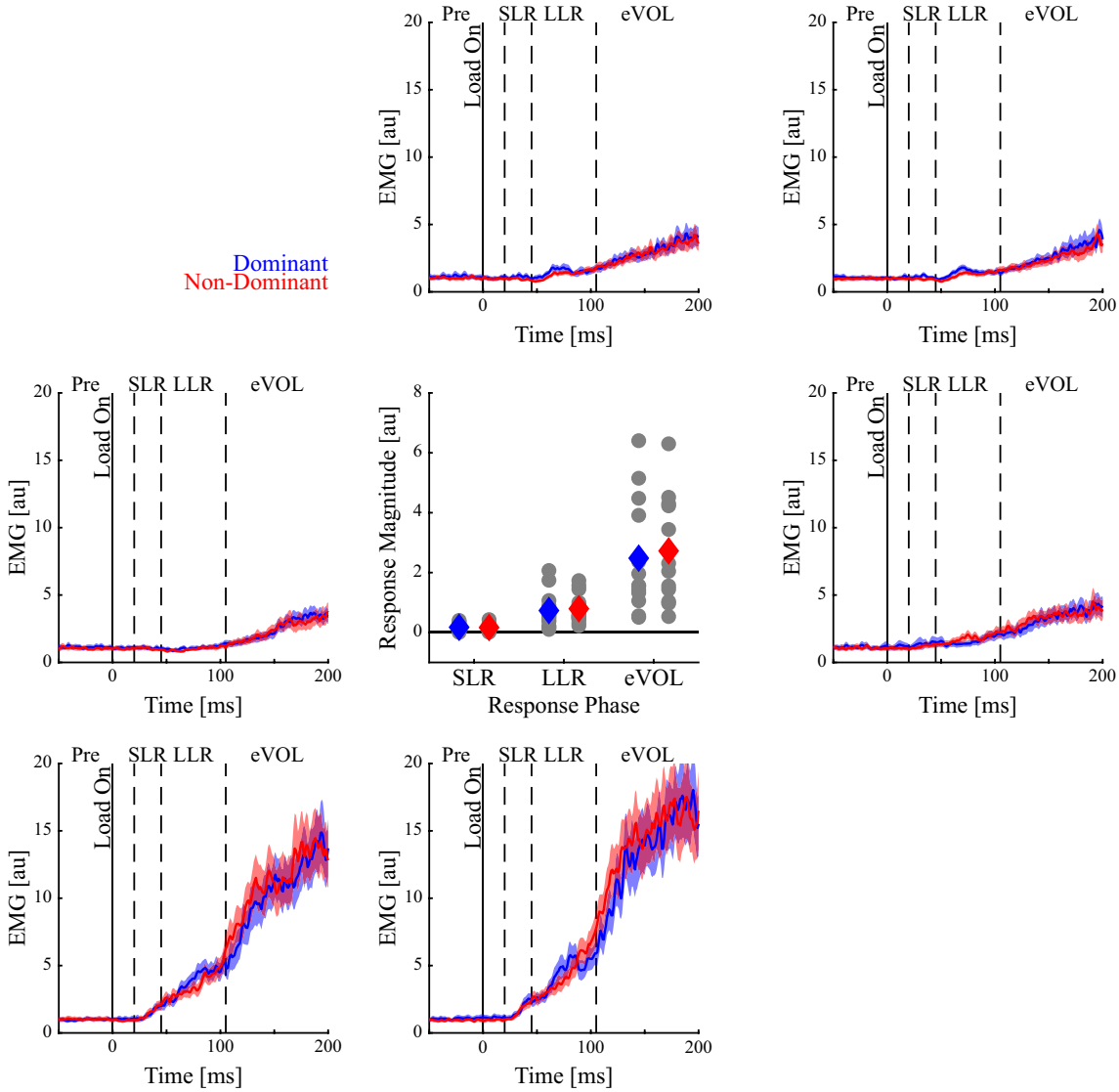

Figure 8. Brachioradialis muscle activity and response magnitude in *experiment 1*. Outside panels represent muscle stretch reflexes for each applied torque and are oriented as in Fig. 2*B*. Colored lines indicate group averages of the dominant (blue) and nondominant (red) arms. Shaded areas indicate ±1 SE. Solid vertical lines indicate perturbation onset. Vertical lines separate phases of the stretch reflex: preperturbation activity (Pre: −50 to 0 ms), short-latency reflex (SLR: 20 to 45 ms), long-latency reflex (LLR: 45 to 105 ms), and early voluntary response (eVOL: 105 to 200 ms). *Center*: the response magnitude. Colored diamonds depict the group average response magnitude across the SLR, LLR, and eVOL time windows. Gray dots represent individual subject data. au, Arbitrary units, EMG, electromyogram.

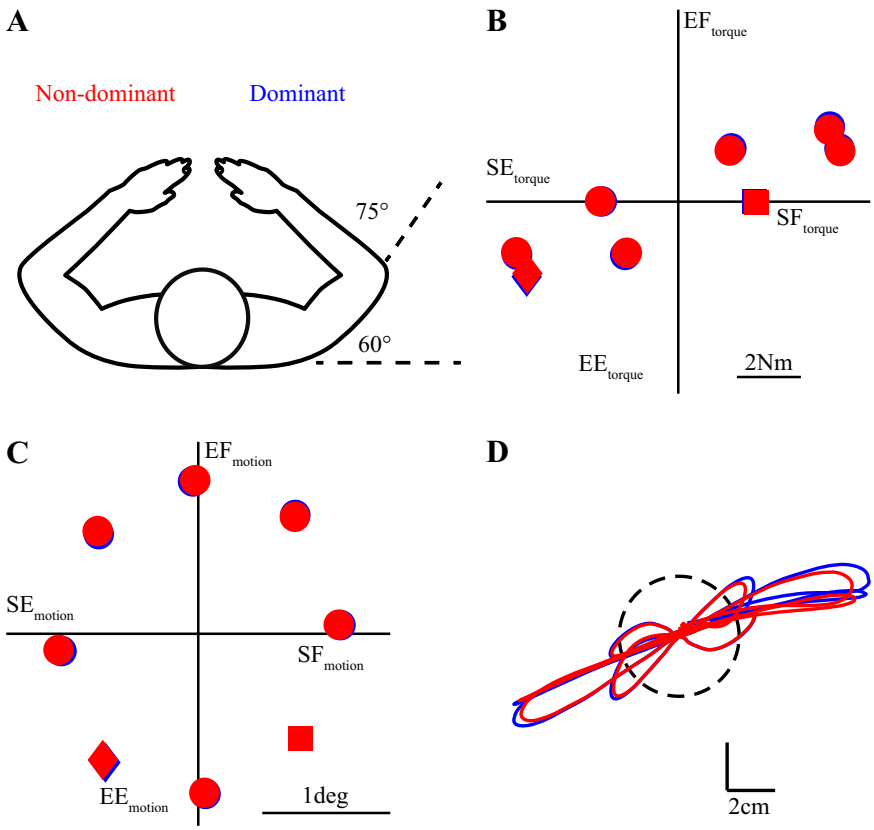

Figure 9. Experimental setup and perturbation-evoked displacements in *experiment 2*. *A*: initial limb configuration of the dominant and nondominant arms in *experiment 2*. *B*: nonuniform distribution of applied torque pulses for the dominant and nondominant arms after estimating limb inertia. We applied combinations of elbow extension (EE), elbow flexion (EF), shoulder extension (SE), and shoulder flexion (SF) torques. *C*: near-uniform angular displacement of the dominant and nondominant arms measured 50 ms after perturbation onset. *D*: group average hand paths for all 8 perturbation directions. Note that the data for the left arm have been reflected about the vertical axis. Dashed circle indicates the outer boundary of the goal target.

(means closer to Θ). Starting in the LLR, the PTDs of the posterior deltoid muscle in both arms were more closely aligned with an internal model of the limb's dynamics (means closer to τ). PTDs of the posterior deltoid did not differ statistically in any time window [SLR: $t(12) = 0.30$, $P = 1.000$, $d = 0.08$; LLR: $t(12) = 1.24$, $P = 0.953$, $d = 0.34$; eVOL: $t(12) = 0.35$, $P = 1.000$, $d = 0.10$].

We compared the response magnitude of the posterior deltoid muscles in the SLR, LLR, and eVOL time windows. The response magnitude provides information about the overall sensitivity of stretch reflexes across all perturbation directions. Provided the arms are displaced similarly and the change in state of the limbs arising from the perturbation is not different, larger response magnitudes would be expected if the nondominant arm is controlled by mechanisms that rely on the modulation of sensory feedback from individual joints to alter the limb's impedance (9–11). There were no statistical differences in the response magnitudes of the posterior deltoid muscles in any time window of the stretch response [SLR: $t(12) = 1.73$, $P = 0.435$, $d = 0.48$; LLR: $t(12) = 0.82$, $P = 1.000$, $d = 0.23$; eVOL: $t(12) = -1.05$, $P = 1.000$, $d = -0.29$].

We performed the same analyses on the stretch reflex of the pectoralis major muscle (Fig. 5 and Fig. 6). No statistical difference was detected in the preperturbation activity of the pectoralis major muscle across the two arms [$t(12) = 1.09$, $P = 1.000$, $d = 0.30$]. The PTDs of the pectoralis major muscle were not statistically different across arms in the SLR [$t(12) = -0.17$, $P = 1.000$, $d = -0.05$], LLR [$t(12) = -0.18$, $P = 1.000$, $d = -0.05$], and eVOL [$t(12) = 2.14$, $P = 0.214$, $d = 0.59$] time windows. Response magnitudes were not statistically different in the SLR [$t(12) = 0.72$, $P = 1.000$, $d = 0.19$] and LLR [$t(12) = 1.95$, $P = 0.300$, $d = 0.54$] time windows. However, the dominant arm displayed a significantly larger response magnitude in the eVOL time window [$t(12) = 3.83$, $P = 0.009$, $d = 1.06$].

Preperturbation activity and stretch reflexes were also compared across the dominant and nondominant brachioradialis and triceps lateral muscles. Preperturbation activity was not statistically different in the triceps lateralis [Fig. 7; $t(12) = 0.53$, $P = 1.000$, $d = 0.15$] or brachioradialis [Fig. 8; $t(12) = 0.63$, $P = 1.000$, $d = 0.17$] muscles when comparing across the two arms. Moreover, the response magnitudes of the elbow muscles were not statistically different in any epoch of the stretch reflex [triceps lateralis: SLR: $t(12) = 0.01$, $P = 1.000$, $d = 0.00$; LLR: $t(12) = 1.59$, $P = 0.553$, $d = 0.44$; eVOL: $t(12) = 1.36$, $P = 0.795$, $d = 0.38$; brachioradialis: SLR: $t(12) = 0.20$, $P = 1.000$, $d = 0.06$; LLR: $t(12) = -0.59$, $P = 1.000$, $d = -0.16$; eVOL: $t(12) = -1.02$, $P = 1.000$, $d = -0.28$].

Experiment 2: Arm Kinematics and Motor Behavior

Behavioral responses and muscle stretch reflexes were relatively consistent across the two arms in *experiment 1*. However, small differences in shoulder and elbow motion began within 50 ms of perturbation onset (12.2–14.3% or 0.055–0.065°). Although small, these differences in limb motion could confound the analysis because of potential differences in afferent feedback arising from the state of the limbs (e.g., position, velocity, and acceleration) (39, 57). Accordingly, we performed a follow-up experiment to control the motion of the shoulder and elbow joints at the

Table 2. *Outcomes of the two-way repeated-measures ANOVAs for motor behavior and applied torques in experiment 2*

Outcome Measure	Effect	*F* Statistics	*P* Value	η^2
Shoulder angle at 50 ms	Hand	F (1,14) = 4.47	0.053	0.004
	Perturbation	F (1.74,24.4) = 6,058.62	4.47e−33	0.996
	Interaction	F (2.04,28.51) = 0.80	0.460	0.016
Elbow angle at 50 ms	Hand	F (1,14) = 2.39	0.144	0.003
	Perturbation	F (1.75,24.53) = 3,843.72	7.82e−31	0.994
	Interaction	F (1.67,23.32) = 0.59	0.533	0.011
Peak hand displacement	**Hand**	F (1,14) = 6.83	0.020	0.044
	Perturbation	F (1.72,24.1) = 258.25	1.90e−16	0.804
	Interaction	F (3.48,48.74) = 3.05	0.031	0.016
Peak joint displacement	Hand	F (1,14) = 2.19	0.161	0.009
	Perturbation	F (1.69,23.6) = 201.94	5.83e−15	0.736
	Interaction	F (2.47,34.62) = 0.85	0.459	0.003
Return time	Hand	F (1,14) = 4.30	0.057	0.014
	Perturbation	F (2.7,37.77) = 56.41	1.67e−13	0.327
	Interaction	F (2.73,37.17) = 0.91	0.437	0.004
End point accuracy	Hand	F (1,14) = 2.61	0.128	0.006
	Perturbation	F (2.6,36.34) = 10.75	6.77e−05	0.185
	Interaction	F (3.28,45.89) = 2.21	0.094	0.009
Linearity of hand paths	Hand	F (1,14) = 0.43	0.524	0.002
	Perturbation	F (3.36,46.99) = 90.05	3.00e−20	0.713
	Interaction	F (3.06,42.81) = 1.75	0.170	0.015
Linearity of joint paths	Hand	F (1,14) = 0.12	0.730	0.000
	Perturbation	F (2.57,35.94) = 70.72	2.17e−14	0.730
	Interaction	F (2.78,38.89) = 0.18	0.900	0.002
Shoulder torque	Hand	F (1,14) = 0.35	0.565	0.000
	Perturbation	F (7,98) = 934.04	1.05e−86	0.983
	Interaction	F (7,98) = 0.48	0.845	0.001
Elbow torque	Hand	F (1,14) = 0.19	0.673	0.000
	Perturbation	F (7,98) = 1296.25	1.38e−93	0.983
	Interaction	F (7,98) = 9.70	3.97e−09	0.027

Statistically significant effects are presented in bold.

onset of the LLR (50 ms after perturbation; Fig. 9*C*, Table 2).

In contrast to *experiment 1*, no statistical differences were exhibited in the linearity of hand paths, joint paths, or peak joint displacements (Table 2). However, the peak hand displacements were statistically different across the arms (Table 2). After decomposing the ANOVA, we found that the nondominant arm was displaced less in two of eight perturbation directions (pure elbow extension and combined elbow and shoulder extension, P = 0.032–0.040, d = 0.85–0.88), whereas no statistical differences were observed in the remaining six perturbation directions (P = 0.384–1.000, d = 0.27–0.56). Note that the differences in behavior may have arisen from the mechanical properties of the arms. In fact, larger elbow torque pulses were required to displace the dominant arm the same distance at 50 ms after perturbation in two of eight perturbation directions (both 4.3% or 0.10 Nm, P = 0.048, d = 0.83; Table 2). We did not observe statistical differences in torque pulses at the shoulder. Return times and end point accuracy were not statistically different between the arms (Table 2).

Experiment 2: Preferred Motion Direction and Response Magnitude

Figure 10 displays the evoked muscle activity of the posterior deltoid for each applied perturbation. The analyses were focused on the PMDs and response magnitudes during the SLR and LLR epochs. The design does not permit direct comparison of normalized preperturbation muscle activity across the arms because the normalization was performed relative to the average activity when holding the background loads before perturbation onset. Similar to previous research (25), the PMDs of the posterior deltoid were close to Θ (single-joint motion) in the SLR time window, whereas the PMDs were close to τ in the LLR time window (Fig. 10 and Fig. 11). The PMDs did not differ statistically within the SLR [t(14) = 0.30, P = 1.000, d = 0.08] or LLR [t(14)=0.27, P = 1.000, d = 0.07] time windows. The response magnitude of the dominant posterior deltoid muscle (Fig. 10 and Fig. 11) was statistically larger in the SLR [t(14)=2.87, p = 0.025, d = 0.74]. There were no statistical differences when comparing response magnitudes in the LLR time window across arms [t(14) = −0.19, P = 1.000, d = −0.05].

PMDs and response magnitudes of the brachioradialis muscle (Fig. 12 and Fig. 13) showed patterns similar to the posterior deltoid. The PMDs were tuned toward Θ in the SLR, whereas the PMDs were tuned to τ in the LLR and no statistical difference was detected in the LLR PMDs [t(14) = 0.75, P = 0.937, d = 0.19]. However, a statistical difference in PMDs was found during the SLR [t(14) = −2.61, P = 0.042, d = −0.67), with the dominant PMD being closer to Θ. The response magnitudes of the brachioradialis muscle did not differ statistically in either reflex epoch [SLR: t(14) = 0.71, P = 0.984, d = 0.18; LLR: t(14) = 1.07, P = 0.607, d = 0.28].

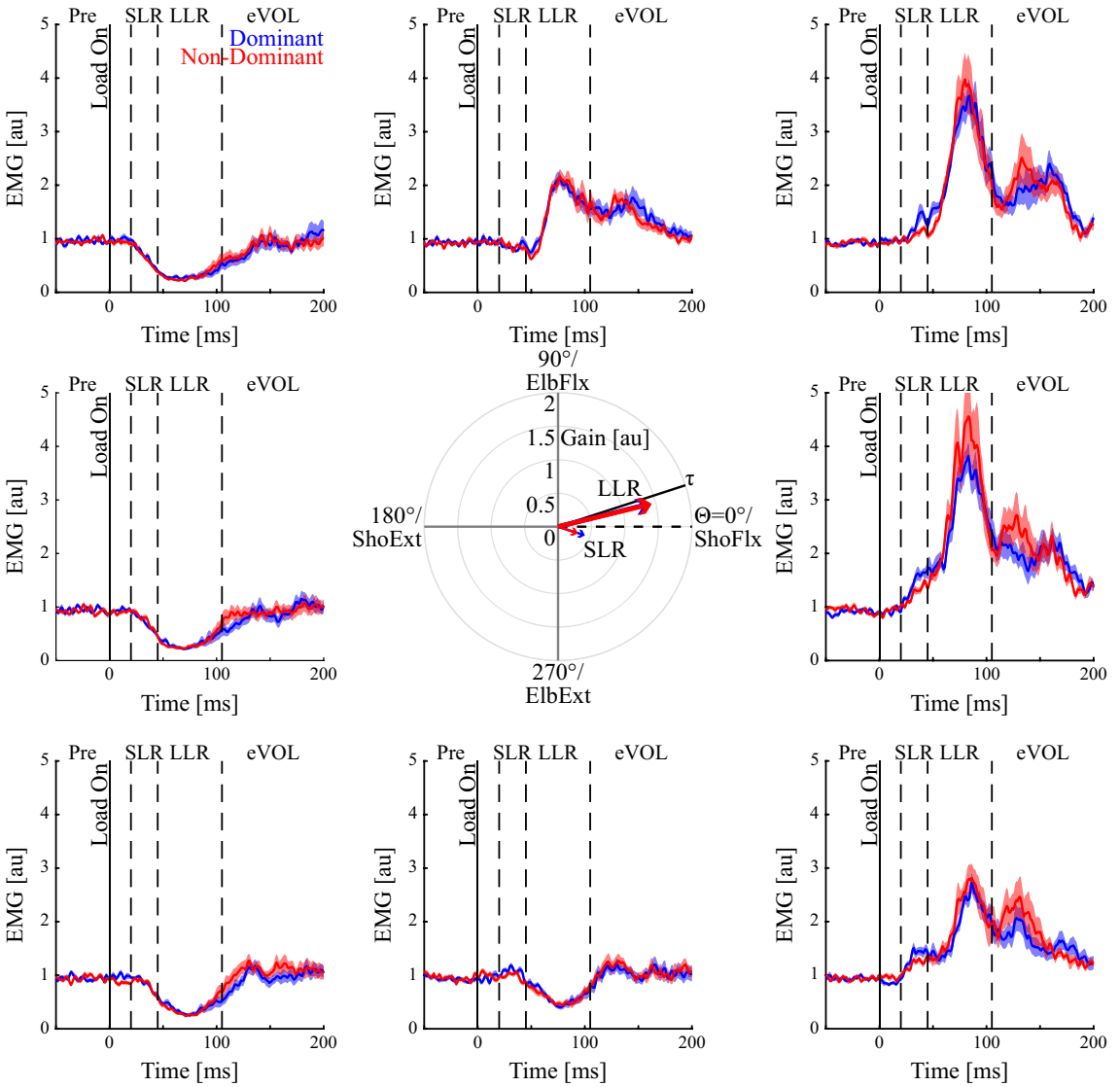

Figure 10. Posterior deltoid muscle activity, preferred motion direction (PMD), and response magnitude in *experiment 2*. Outside panels display stretch reflexes based on near-uniform elbow and shoulder angle displacements. The panels are oriented as in Fig. 9C. Colored lines indicate group averages of the dominant (blue) and nondominant (red) arms. Shaded areas indicate ±1 SE. Solid vertical lines indicate perturbation onset. Dashed vertical lines separate phases of the stretch reflex: preperturbation activity (Pre: −50 to 0 ms), short-latency reflex (SLR: 20 to 45 ms), long-latency reflex (LLR: 45 to 105 ms), and early voluntary response (eVOL: 105 to 200 ms). *Center*: a polar plot of the average PMDs and response magnitudes of posterior deltoid stretch reflexes. The thin arrows reflect the PMD and response magnitude during the SLR. The thick arrows indicate the PMD and response magnitude during the LLR. The dashed black line corresponds to the local PMD (Θ). The solid black line corresponds to the ideal PMD (τ). au, Arbitrary units; ElbExt, elbow extension; ElbFlx, elbow flexion; EMG, electromyogram; ShoExt, shoulder extension; ShoFlx, shoulder flexion.

Control Comparisons

Preperturbation muscle activity in *experiment 2* could not be compared directly across the arms because of the normalization procedure. Therefore, it is not possible to rule out differences in preperturbation muscle activity that could systematically alter the impedance of the arm. As an internal control, we compared the unnormalized muscle activity across all time windows and muscles. Similar to the normalized data, no statistical differences were observed in reflexive muscle activity between the dominant and nondominant arms. Note, however, that comparisons of unnormalized muscle activity should be interpreted with caution (see DISCUSSION for further details).

Combined Experiments: Correlations of Motor Behavior and Stretch Reflexes between the Dominant and Nondominant Arms

Because of the similarity of outcome measures across the two arms, we investigated the relationship in motor behavior, PTDs/PMDs, and response magnitudes between the dominant and nondominant arms. Pearson's product moment correlations were used to quantify the relationship between peak hand and joint displacements, return times, hand and joint path linearity, and end point accuracy across the arms. Motor behavior was averaged across perturbation directions. Correlations were also calculated between PTDs/PMDs and

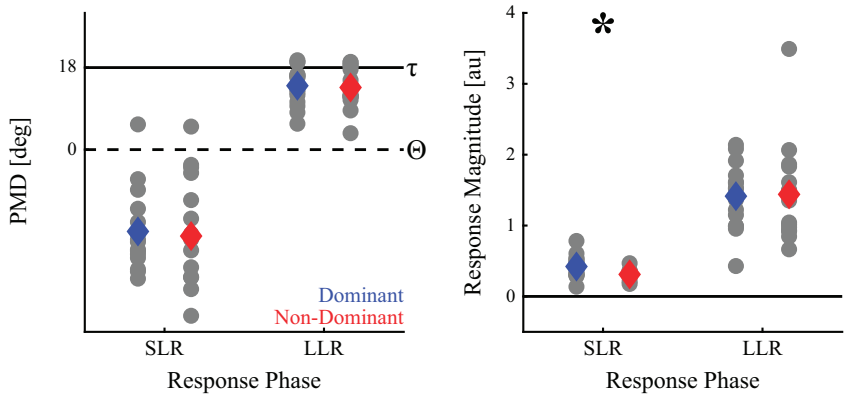

Figure 11. Preferred motion direction (PMD) and response magnitude of posterior deltoid stretch reflexes in *experiment 2*. Colored diamonds depict the group average PMDs and response magnitude of the dominant (blue) and nondominant (red) shoulder extensors across the short-latency reflex (SLR) and long-latency reflex (LLR) time windows. Gray dots represent individual subject data. Dashed black line corresponds to the local PMD (Θ). Solid black line corresponds to the ideal PMD (τ). au, Arbitrary units. $*P < 0.05$.

response magnitudes of the posterior deltoid LLRs and the response magnitude of LLRs in the brachioradialis muscle (Fig. 14). The two arms showed strong positive correlations in kinematic responses to the perturbations ($r \geq 0.69$, $P < 0.001$), a moderate positive correlation in PTDs/PMDs ($r = 0.43$, $P = 0.013$), and strong positive correlations in response magnitudes of the posterior deltoid ($r = 0.57$, $P < 0.001$) and brachioradialis muscles ($r = 0.66$, $P < 0.001$). The correlations in outcomes of the two arms suggest that stretch reflexes evoked by sudden imposed loads during postural control are similar in the dominant and nondominant arms.

DISCUSSION

Summary

A prominent hypothesis in the field of sensorimotor control is that the nervous system uses specialized mechanisms for controlling the dominant and nondominant arms. It has been proposed that the dominant hemisphere leverages an internal model of limb dynamics to produce efficient movements, whereas the nondominant hemisphere relies on impedance mechanisms through sensitive but local modulation of sensory feedback to control static arm postures (9–11). We tested this hypothesis in terms of stretch reflexes evoked by mechanical loads during postural control (24, 25). The approach allowed us to examine how well the directional sensitivity of each arm's responses reflected the intrinsic dynamics of the arm (reflecting an internal model) and overall sensitivity to limb displacement (reflecting impedance control). In most comparisons, we found no statistical differences but moderate to strong correlations in the internal model of limb dynamics and sensitivity to muscle stretch when comparing responses across the two arms. Collectively, the results do not support the idea that the dominant arm specializes in the use of internal models and the nondominant arm in impedance control through elevated reflex gains when countering sudden loads imposed during upper limb posture control.

Similar Internal Model of Limb Dynamics between the Dominant and Nondominant Arms during Posture Control

Previous studies have shown that the reflexes of upper limb muscles are sensitive to local joint motion during the SLR but account for the motion of other joints in the LLR (24–27). Likewise, we found that the PTDs and PMDs of shoulder and elbow muscles in both arms accounted for limb dynamics in the LLR time window. In contrast, the SLR typically reflected local joint motion. Note that a statistical difference in the PMDs of the brachioradialis muscle was observed in the SLR time window in *experiment 2*. This difference is likely caused by small imperfections in enforcing uniform joint motion when disturbing the arm in different directions (Fig. 9*C*). Overall, the PMDs of both arms were more closely aligned with sensitivity to single-joint motion (aligned with Θ; Fig. 12 and Fig. 13) than they were aligned with multijoint motion reflecting an internal model of limb dynamics (alignment with τ). The statistical difference was caused by the PMD of the SLR being more closely aligned with single-joint motion in the dominant brachioradialis muscle. A moderate positive correlation was observed in the PTDs and PMDs of the shoulder muscles in the LLR time window. Thus, we argue that the internal model of limb dynamics that was utilized by stretch reflexes during postural control was similar across the arms.

Similar Roles of Sensory Feedback in the Dominant and Nondominant Arms during Posture Control

Behavioral outcomes and response magnitudes were used to investigate differences in controlling the posture of the dominant and nondominant arms. In both experiments, return times and end point accuracy did not differ statistically between the two arms. The behavioral responses were variable across participants, yet strongly correlated across the arms. Specifically, individuals who were displaced farther by the perturbation, had longer return times, had more linear hand and joint paths, or had higher end point accuracy tended to display similar behavior with both arms (Fig. 14).

In contrast to the idea of hemispheric specialization (9–11), response magnitudes were not statistically larger in the nondominant arm. In fact, the response magnitude was elevated in the dominant pectoralis major muscle within the eVOL time window in *experiment 1*. The nature of the torque combinations produced larger elbow joint displacements (Fig. 2*C*), such that differences in pectoralis major activity would have less influence on behavioral outcomes compared with the activity of the elbow muscles. This may explain why we did not observe statistical differences in peak hand displacements across the arms. In *experiment 2*, the dominant posterior deltoid displayed elevated responses in the SLR time window. The small amplitude and brief

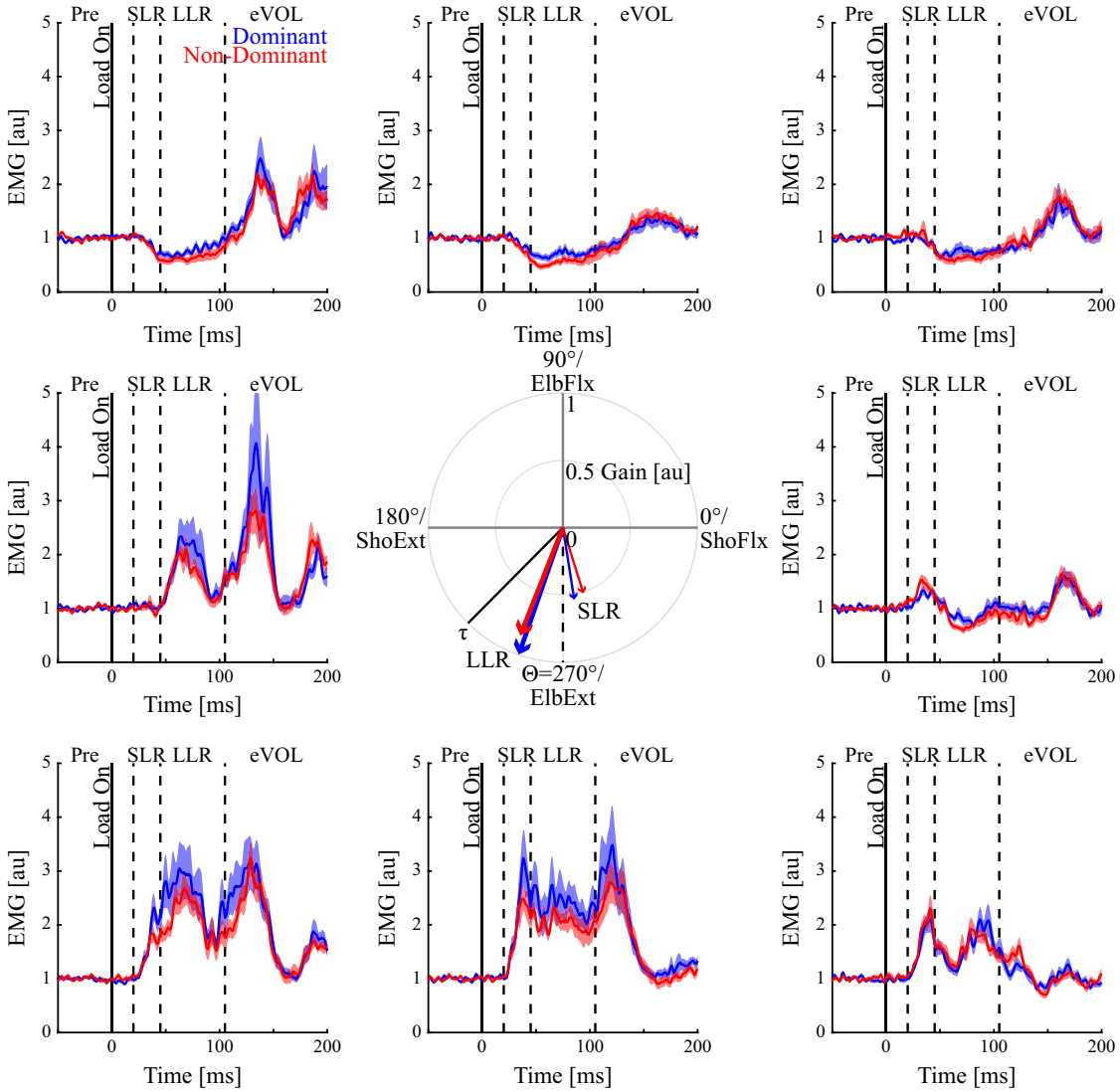

Figure 12. Brachioradialis muscle activity, preferred motion direction (PMD), and response magnitude in *experiment 2*. Outside panels display muscle stretch reflexes based on near-uniform angular displacements of the elbow and shoulder joints. The panels are oriented as in Fig. 9C. Colored lines indicate group averages of the dominant (blue) and nondominant (red) arms. Shaded areas indicate ±1 SE. Solid vertical lines indicate perturbation onset. Dashed vertical lines separate phases of the stretch reflex: preperturbation activity (Pre: −50 to 0 ms), short-latency reflex (SLR: 20 to 45 ms), long-latency reflex (LLR: 45 to 105 ms), and early voluntary response (eVOL: 105 to 200 ms). *Center*: a polar plot of the average PMDs and response magnitude of brachioradialis stretch reflexes. The thin arrows reflect the PMD and response magnitude during the SLR. The thick arrows indicate the PMD and response magnitude during the LLR. The dashed black line corresponds to the local PMD (Θ). The solid black line corresponds to the ideal PMD (τ). au, Arbitrary units; ElbExt, elbow extension; ElbFlx, elbow flexion; EMG, electromyogram; ShoExt, shoulder extension; ShoFlx, shoulder flexion.

duration of the SLR compared with the LLR may explain why there were no corresponding statistical differences in behavioral measures, including peak joint displacements, return times, end point accuracy, or the linearity of hand and joint paths.

Another possible explanation is that the biarticular muscles were upregulated to increase the impedance of the nondominant arm (58). In agreement with this idea, Walker and Perreault (36) showed a selective increase in the background activity and stretch responses of the biarticular muscles when countering postural perturbations with the nondominant arm. However, when controlling for differences in background muscle activity in the analysis, there were no statistical differences in biarticular stretch reflexes between the two arms. When the analysis was restricted to younger adults who were closer in age to our sample, Walker and Perreault (36) observed statistically increased long-latency stretch reflexes in the monoarticular elbow muscles in the nondominant arm. Although it is possible that the biarticular muscles were selectively upregulated in the nondominant arm in our study, the effect sizes for differences in the stretch reflexes of the monoarticular muscles were generally of small to moderate amplitude, with the exception of the effects noted above. Some muscles displayed larger responses in the dominant arm and others in the nondominant arm. In short, the lack of consistent differences in directional tuning (internal model) and variable gains of muscle responses (response magnitudes), both within and across the arms, does not

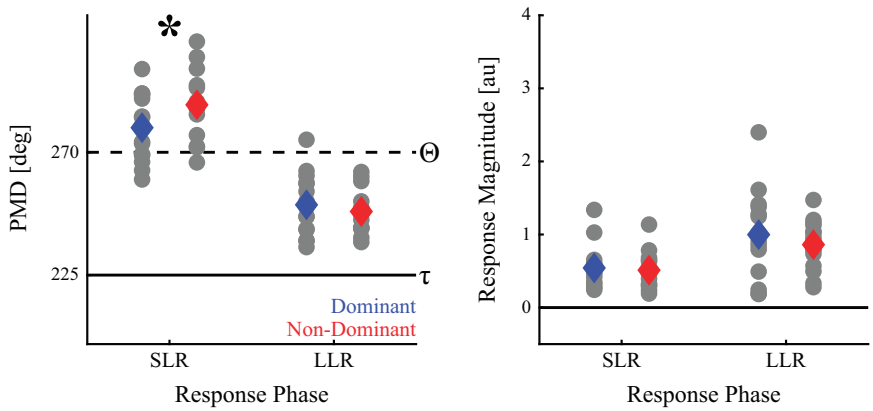

Figure 13. Preferred motion direction (PMD) and response magnitude of brachioradialis stretch reflexes in *experiment 2*. Colored diamonds depict the group average PMDs and response magnitude of the dominant (blue) and nondominant (red) elbow flexors across the short-latency reflex (SLR) and long-latency reflex (LLR) time windows. Gray dots represent individual subject data. Dashed black line corresponds to the local PMD (Θ). Solid black line corresponds to the ideal PMD (τ). au, Arbitrary units. $*P < 0.05$.

provide clear evidence that reflexes are specialized in posture control.

In line with the strong correlations observed in behavioral outcomes, strong positive correlations were found between the response magnitudes of the posterior deltoid and brachioradialis stretch reflexes across the arms, such that individuals tended to display similar sensitivity to muscle stretch with both arms. Similar results were also obtained when examining the unnormalized muscle activity. Although there is no gold standard for normalizing muscle activity, a recent consensus paper cautioned against comparing unnormalized muscle activity because of factors related to electrode placement and impedance of the recordings that may influence the amplitude and quality of EMG signals (59). However, Besomi and colleagues (59) also noted that unnormalized muscle activity can be used to assess whether findings are robust after other normalization procedures. We compared unnormalized muscle activity in *experiment 2* to rule out systematic differences in preperturbation muscle activity that could arise, for example, if the nervous system used tonic coactivation to alter the impedance of the nondominant arm. Although electrode placement, skin preparation, and amplification were standardized to the best of our abilities to mitigate differences in muscle recordings, the results should nevertheless be interpreted with caution. Normalizing the muscle activity to reference loads (as used in *experiment 1*) would mitigate this limitation.

Note that the magnitudes of the short- and long-latency reflexes were elevated, and early voluntary responses muted, when comparing responses in *experiment 2* with *experiment 1*. These differences are expected, as they arise from the background loads used to preexcite the motor neuron pool and amplify reflex responses in *experiment 2* (37–39, 54). Despite differences in the size of the responses across the two experiments, the relative scaling of reflexes across the dominant and nondominant arms was qualitatively similar. This effect was evident when we transformed the data within each experiment, pooled the responses across the two experiments, and found a strong positive correlation in the magnitude of posterior deltoid and brachioradialis responses across the two arms (Fig. 14). Finally, the amplitude of the early voluntary response was muted when comparing the results of *experiment 2* with *experiment 1*. The difference in early voluntary responses is expected because of the duration of the torque pulse perturbations in *experiment 2* (80 ms), which can cause a pronounced downregulation of muscle activity within ~30 ms of the offset of torque perturbations of amplitude similar to the perturbations used in *experiment 2* (53, 60). Collectively, the behavioral data and muscle signatures of feedback control suggest that the nervous system uses similar feedback gains to control the posture of the dominant and nondominant arms.

Comparisons to Previous Paradigms

To our knowledge, past studies have focused on the response magnitude of stretch reflexes in bimanual tasks (61–63), interlimb differences in responding to tendon taps at the wrist (64) or perturbations applied at the elbow (36). Although these data provide insight on the response magnitude of stretch reflexes in controlling the arms or their coordination, they do not permit direct comparison of the internal model of limb dynamics across the two arms. For example, Aimonetti et al. (64) observed greater stretch reflexes in the dominant wrist in the absence of difference in H reflexes, whereas Walker and Perreault (36) observed greater stretch reflexes in the nondominant elbow muscles during a posture control task. One possible explanation for Walker and Perreault's findings (36) is that the authors preloaded elbow muscles in the direction of the impending perturbation, which may modulate long-latency reflexes in posture control even in the absence of differences in background activity (65, 66). Individuals in our experiments countered six (*experiment 1*) or eight (*experiment 2*) different torque perturbations in block-randomized order. When present in *experiment 2*, the background loads preexcited the brachioradialis and posterior deltoid muscles but did not cue the direction of the perturbation. Collectively, the experimental design may have limited the ability to use specific strategies to anticipate and counter the perturbations with the nondominant arm.

Another possible explanation is the nature of the posture tasks in our experiments. Participants were required to return their hand to the start position within a specified time window when displaced by the perturbation (500 ms). Previous studies did not impose an explicit task goal (64), or participants were instructed not to resist the perturbations

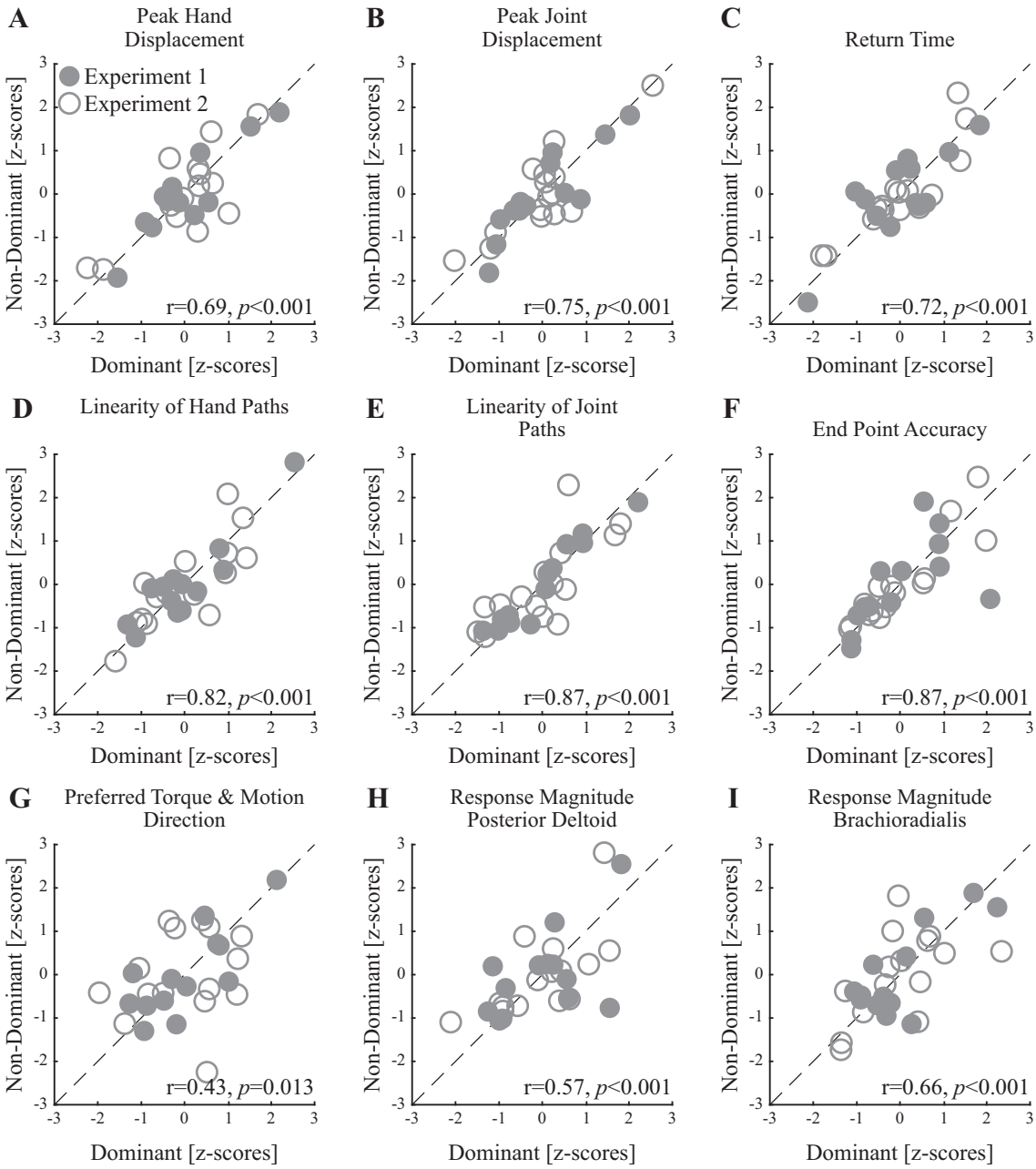

Figure 14. Correlations of motor behavior and stretch reflexes between the dominant and nondominant arms. Panels display standardized outcomes of the dominant (*x*-axis) and nondominant (*y*-axis) arms for peak hand displacements (*A*), peak joint displacements (*B*), return times (*C*), linearity of hand paths (*D*), linearity of joint paths (*E*), end point accuracy (*F*), preferred torque direction (*experiment 1*) and preferred motion direction of the posterior deltoid muscle in the long-latency reflex (LLR) time window (*G*), response magnitude of the posterior deltoid muscle in the LLR time window (*H*), and response magnitude of the brachioradialis muscle in the LLR time window (*I*). The data were averaged across all perturbations for each individual. Filled circles indicate individual data points for *experiment 1*. Open circles indicate individual data points for experiment 2. Dashed black line displays unity.

and did not have to return to the target to complete the trial (36). The nervous system is capable of altering feedback control and generating flexible responses to accommodate different task demands (67, 68). This flexibility has been observed when comparing the amplitude of long-latency reflexes in the dominant arm between tasks with different timing demands (41, 45), locations and shapes of the behavioral goal (48, 69), obstacles in the environment (70), and coordination across the arms (61–63, 71, 72). Goal-directed responses seem to rely on activity in the primary motor cortex (73–76), cerebellum (77), and primary somatosensory cortex (78, 79). The dorsal premotor area may also be involved in setting the gain of long-latency reflexes. A recent study demonstrated that cooling the dorsal premotor area reduces the gain of feedback responses and leads to larger limb displacements in monkeys (40). Each of these areas projects to the spinal cord and influences its excitability during voluntary motor actions. Collectively, these mechanisms may serve to alter the control of goal-directed motor actions.

Motor Behavior Is Influenced by Differences in Limb Inertia

We employed two different protocols to investigate how individuals countered mechanical perturbations during upper limb posture control. We applied the same mechanical perturbations at both arms in *experiment 1*, whereas we evoked the same joint motion shortly after perturbation onset in both arms in *experiment 2*. We did not observe statistical differences in end point accuracy or in return times between the two arms. In our first experiment, there were small but quantifiable differences in elbow and shoulder joint motion at 50 ms after perturbation onset. The differences in joint motion reduced the linearity of hand and joint paths when the nondominant arm was displaced by the same perturbation. The differences in initial displacement were too early to reflect sensory feedback when factoring in conduction delays (74), the transformation from muscle activity to force production (80, 81), and motion of the limb (30, 51). Instead, we argue that these differences reflect inertial properties of the limb that dominate initial motion after a perturbation (39, 82).

In view of these limitations, we performed a second experiment in which we applied torque pulses that elicited prescribed patterns of joint motion and accounted for differences in limb inertia (25). The approach enabled more precise control over limb motion until the onset of the long-latency reflex (50 ms after perturbation) and eliminated any statistical differences in the linearity of hand paths and joint paths caused by the perturbations. However, the differences in limb inertia meant that larger elbow joint torques were required to displace the arms the same distance at 50 ms after perturbation. As a result, the applied torques produced a small, but statistically significant increase in the peak hand displacement of the dominant arm. Our findings are consistent with studies that reported greater bone mineral density (83), longer and heavier humeri (84), and larger mass in the dominant arm (85) and a reduction in muscle area in the nondominant forearm (86). Collectively, these morphological differences may increase the inertia of the dominant arm (87) and cause the small but quantifiable differences in limb motion observed in our first experiment.

Posture Control versus Reaching Movements

A potential limitation of our study is that we only examined how the nervous system attempts to maintain the posture of the dominant and nondominant arms. Indeed, past studies suggest that M1 neurons spontaneously change their load sensitivity during the transition from posture to movement, which suggests that the two tasks involve different control mechanisms (88). Recent research has also introduced the idea of serial hybrid control to understand how the nervous system controls reaching movements in the dominant and nondominant arms. The framework suggests that the nervous system initiates movement with both arms relying on an internal model of limb dynamics and switches to impedance control to attain and hold the goal target (89, 90). After initiating the reach, the nervous system may more rapidly switch to controlling the impedance of the nondominant arm, presumably by increasing the gains on sensory feedback (89, 90). Further research supports the idea that separate mechanisms are involved in controlling reaching movements versus maintaining a static posture at the movement end point (91, 92). The proposed framework might apply to self-initiated movements and not transfer to stretch reflexes in posture control. However, recent studies have reported similar adaptation of internal models when reaching independently with each arm in the presence of force fields (93, 94). It seems that the nervous system can adapt equally well to novel loads with either arm (93) and that interlimb transfer of motor adaptation is bidirectional between the arms (94). Taken together, our results in combination with recent studies suggest that differences in controlling the two arms may be task dependent and could be further addressed by future studies.

Conclusions

In summary, our findings reveal similar behavioral responses and stretch reflexes to sudden loads imposed when controlling the posture of the dominant and nondominant arms. Further research is required to understand in which contexts the nervous system might use different modulation of behavioral responses and stretch reflexes to control the posture and movement of the upper limbs.

GRANTS

This work was supported by the Natural Sciences and Engineering Research Council of Canada (NSERC) Discovery Grant (2017-04829), University of Calgary-Faculty of Kinesiology, and Calgary Health Trust awarded to T.C. P.M. is supported by an Eyes High Doctoral Recruitment Scholarship of the University of Calgary.

DISCLOSURES

No conflicts of interest, financial or otherwise, are declared by the authors.

AUTHOR CONTRIBUTIONS

P.M., I.K., and T.C. conceived and designed research; P.M., I.K., R.A., and T.C. performed experiments; P.M. and T.C. analyzed data; P.M., I.K., and T.C. interpreted results of experiments; P.M. and T.C. prepared figures; P.M. and T.C. drafted manuscript; P.M., I.K., and T.C. edited and revised manuscript; P.M., I.K., and T.C. approved final version of manuscript.

REFERENCES

1. **Papadatou-Pastou M**, **Ntolka E**, **Schmitz J**, **Martin M**, **Munafò MR**, **Ocklenburg S**, **Paracchini S.** Human handedness: a meta-analysis. *Psychol Bull* 146: 481–524, 2020. doi:10.1037/bul0000229.
2. **Marcori AJ**, **Okazaki VH.** A historical, systematic review of handedness origins. *Laterality* 25: 87–108, 2020. doi:10.1080/1357650X.2019.1614597.
3. **Hepper PG**, **Shahidullah S**, **White R.** Handedness in the human fetus. *Neuropsychologia* 29: 1107–1111, 1991. doi:10.1016/0028-3932(91)90080-r.
4. **Hepper PG**, **Wells DL**, **Lynch C.** Prenatal thumb sucking is related to postnatal handedness. *Neuropsychologia* 43: 313–315, 2005. doi:10.1016/j.neuropsychologia.2004.08.009.
5. **Budisavljevic S**, **Castiello U**, **Begliomini C.** Handedness and white matter networks. *The Neuroscientist* 27: 88–103, 2021. doi:10.1177/1073858420937657.
6. **Broca P.** Remarques sur le siège de la faculté du langage articulé, suivies d'une observation d'aphémie (perte de la parole) [Remarks on the seat of the faculty of articulated language, following an

observation of aphemia (loss of speech)] [Online]. *Bull Soc Anat* 6: 330–357, 1861. https://pure.mpg.de/rest/items/item_2301213/component/file_2452907/content.
7. **Berker EA**, **Berker AH**, **Smith A.** Translation of Broca's 1865 report. Localization of speech in the third left frontal convolution. *Arch Neurol* 43: 1065–1072, 1986. doi:10.1001/archneur.1986.00520100069017.
8. **Pujol J**, **Deus J**, **Losilla JM**, **Capdevila A.** Cerebral lateralization of language in normal left-handed people studied by functional MRI. *Neurology* 52: 1038–1043, 1999. doi:10.1212/wnl.52.5.1038.
9. **Sainburg RL.** Handedness: differential specializations for control of trajectory and position. *Exerc Sport Sci Rev* 33: 206–213, 2005. doi:10.1097/00003677-200510000-00010.
10. **Sainburg RL.** Convergent models of handedness and brain lateralization. *Front Psychol* 5: 1092, 2014. doi:10.3389/fpsyg.2014.01092.
11. **Sainburg RL.** Laterality of basic motor control mechanisms: different roles of the right and left brain hemispheres. In: *Laterality in Sports: Theories and Applications*, edited by Loffing F, Hagemann N, Strauss B, MacMahon C. London: Elsevier, 2016, p. 155–177.
12. **Sainburg RL**, **Kalakanis D.** Differences in control of limb dynamics during dominant and nondominant arm reaching. *J Neurophysiol* 83: 2661–2675, 2000. doi:10.1152/jn.2000.83.5.2661.
13. **Bagesteiro LB**, **Sainburg RL.** Nondominant arm advantages in load compensation during rapid elbow joint movements. *J Neurophysiol* 90: 1503–1513, 2003. doi:10.1152/jn.00189.2003.
14. **Sainburg RL.** Evidence for a dynamic-dominance hypothesis of handedness. *Exp Brain Res* 142: 241–258, 2002. doi:10.1007/s00221-001-0913-8.
15. **Duff SV**, **Sainburg RL.** Lateralization of motor adaptation reveals independence in control of trajectory and steady-state position. *Exp Brain Res* 179: 551–561, 2007. doi:10.1007/s00221-006-0811-1.
16. **Mutha PK**, **Sainburg RL**, **Haaland KY.** Critical neural substrates for correcting unexpected trajectory errors and learning from them. *Brain* 134: 3647–3661, 2011. doi:10.1093/brain/awr275.
17. **Mutha PK**, **Sainburg RL**, **Haaland KY.** Left parietal regions are critical for adaptive visuomotor control. *J Neurosci* 31: 6972–6981, 2011. doi:10.1523/JNEUROSCI.6432-10.2011.
18. **Mani S**, **Mutha PK**, **Przybyla A**, **Haaland KY**, **Good DC**, **Sainburg RL.** Contralesional motor deficits after unilateral stroke reflect hemisphere-specific control mechanisms. *Brain* 136: 1288–1303, 2013. doi:10.1093/brain/aws283.
19. **Naito E**, **Roland PE**, **Grefkes C**, **Choi HJ**, **Eickhoff S**, **Geyer S**, **Zilles K**, **Ehrsson HH.** Dominance of the right hemisphere and role of area 2 in human kinesthesia. *J Neurophysiol* 93: 1020–1034, 2005. doi:10.1152/jn.00637.2004.
20. **Goble DJ**, **Lewis CA**, **Brown SH.** Upper limb asymmetries in the utilization of proprioceptive feedback. *Exp Brain Res* 168: 307–311, 2006. doi:10.1007/s00221-005-0280-y.
21. **Goble DJ**, **Brown SH.** Upper limb asymmetries in the matching of proprioceptive versus visual targets. *J Neurophysiol* 99: 3063–3074, 2008. doi:10.1152/jn.90259.2008.
22. **Scott SH**, **Cluff T**, **Lowrey CR**, **Takei T.** Feedback control during voluntary motor actions. *Curr Opin Neurobiol* 33: 85–94, 2015. doi:10.1016/j.conb.2015.03.006.
23. **Scott SH.** The computational and neural basis of voluntary motor control and planning. *Trends Cogn Sci* 16: 541–549, 2012. doi:10.1016/j.tics.2012.09.008.
24. **Kurtzer IL**, **Pruszynski JA**, **Scott SH.** Long-latency reflexes of the human arm reflect an internal model of limb dynamics. *Curr Biol* 18: 449–453, 2008. doi:10.1016/j.cub.2008.02.053.
25. **Kurtzer I**, **Meriggi J**, **Parikh N**, **Saad K.** Long-latency reflexes of elbow and shoulder muscles suggest reciprocal excitation of flexors, reciprocal excitation of extensors, and reciprocal inhibition between flexors and extensors. *J Neurophysiol* 115: 2176–2190, 2016. doi:10.1152/jn.00929.2015.
26. **Kurtzer I**, **Trautman P**, **Rasquinha RJ**, **Bhanpuri NH**, **Scott SH**, **Bastian AJ.** Cerebellar damage diminishes long-latency responses to multijoint perturbations. *J Neurophysiol* 109: 2228–2241, 2013. doi:10.1152/jn.00145.2012.
27. **Kurtzer I**, **Pruszynski JA**, **Scott SH.** Long-latency responses during reaching account for the mechanical interaction between the shoulder and elbow joints. *J Neurophysiol* 102: 3004–3015, 2009. doi:10.1152/jn.00453.2009.
28. **Weiler J**, **Saravanamuttu J**, **Gribble PL**, **Pruszynski JA.** Coordinating long-latency stretch responses across the shoulder, elbow, and wrist during goal-directed reaching. *J Neurophysiol* 116: 2236–2249, 2016. doi:10.1152/jn.00524.2016.
29. **Weiler J**, **Gribble PL**, **Pruszynski JA.** Goal-dependent modulation of the long-latency stretch response at the shoulder, elbow, and wrist. *J Neurophysiol* 114: 3242–3254, 2015. doi:10.1152/jn.00702.2015.
30. **Maeda RS**, **Cluff T**, **Gribble PL**, **Pruszynski JA.** Compensating for intersegmental dynamics across the shoulder, elbow, and wrist joints during feedforward and feedback control. *J Neurophysiol* 118: 1984–1997, 2017. doi:10.1152/jn.00178.2017.
31. **Wagner MJ**, **Smith MA.** Shared internal models for feedforward and feedback control. *J Neurosci* 28: 10663–10673, 2008. doi:10.1523/JNEUROSCI.5479-07.2008.
32. **Ahmadi-Pajouh MA**, **Towhidkhah F**, **Shadmehr R.** Preparing to reach: selecting an adaptive long-latency feedback controller. *J Neurosci* 32: 9537–9545, 2012. doi:10.1523/JNEUROSCI.4275-11.2012.
33. **Cluff T**, **Scott SH.** Rapid feedback responses correlate with reach adaptation and properties of novel upper limb loads. *J Neurosci* 33: 15903–15914, 2013. doi:10.1523/JNEUROSCI.0263-13.2013.
34. **Maeda RS**, **Cluff T**, **Gribble PL**, **Pruszynski JA.** Feedforward and feedback control share an internal model of the arm's dynamics. *J Neurosci* 38: 10505–10514, 2018. doi:10.1523/JNEUROSCI.1709-18.2018.
35. **Maeda RS**, **Gribble PL**, **Pruszynski JA.** Learning new feedforward motor commands based on feedback responses. *Curr Biol* 30: 1941–1948.e3, 2020. doi:10.1016/j.cub.2020.03.005.
36. **Walker EH**, **Perreault EJ.** Arm dominance affects feedforward strategy more than feedback sensitivity during a postural task. *Exp Brain Res* 233: 2001–2011, 2015. doi:10.1007/s00221-015-4271-3.
37. **Bedingham W**, **Tatton WG.** Dependence of EMG responses evoked by imposed wrist displacements on pre-existing activity in the stretched muscles. *Can J Neurol Sci* 11: 272–280, 1984. doi:10.1017/s0317167100045534.
38. **Matthews PB.** Observations on the automatic compensation of reflex gain on varying the pre-existing level of motor discharge in man. *J Physiol* 374: 73–90, 1986. doi:10.1113/jphysiol.1986.sp016066.
39. **Pruszynski JA**, **Kurtzer I**, **Lillicrap TP**, **Scott SH.** Temporal evolution of "automatic gain-scaling". *J Neurophysiol* 102: 992–1003, 2009. doi:10.1152/jn.00085.2009.
40. **Takei T**, **Lomber SG**, **Cook DJ**, **Scott SH.** Transient deactivation of dorsal premotor cortex or parietal area 5 impairs feedback control of the limb in macaques. *Curr Biol* 31: 1476–1487.e5, 2021. doi:10.1016/j.cub.2021.01.049.
41. **Crevecoeur F**, **Kurtzer I**, **Bourke T**, **Scott SH.** Feedback responses rapidly scale with the urgency to correct for external perturbations. *J Neurophysiol* 110: 1323–1332, 2013. doi:10.1152/jn.00216.2013.
42. **Oldfield RC.** The assessment and analysis of handedness: the Edinburgh Inventory. *Neuropsychologia* 9: 97–113, 1971. doi:10.1016/0028-3932(71)90067-4.
43. **Scott SH.** Apparatus for measuring and perturbing shoulder and elbow. *J Neurosci Methods* 89: 119–127, 1999. doi:10.1016/s0165-0270(99)00053-9.
44. **Singh K**, **Scott SH.** A motor learning strategy reflects neural circuitry for limb control. *Nat Neurosci* 6: 399–403, 2003. doi:10.1038/nn1026.
45. **Cluff T**, **Scott SH.** Apparent and actual trajectory control depend on the behavioral context in upper limb motor tasks. *J Neurosci* 35: 12465–12476, 2015. doi:10.1523/JNEUROSCI.0902-15.2015.
46. **Crevecoeur F**, **Scott SH.** Beyond muscles stiffness: importance of state-estimation to account for very fast motor corrections. *PLoS Comput Biol* 10: e1003869, 2014. [Erratum in *PLoS Comput Biol* 10: e1003996, 2014]. doi:10.1371/journal.pcbi.1003869.
47. **Bagesteiro LB**, **Sainburg RL.** Handedness: dominant arm advantages in control of limb dynamics. *J Neurophysiol* 88: 2408–2421, 2002. doi:10.1152/jn.00901.2001.
48. **Pruszynski JA**, **Kurtzer I**, **Scott SH.** Rapid motor responses are appropriately tuned to the metrics of a visuospatial task. *J Neurophysiol* 100: 224–238, 2008. doi:10.1152/jn.90262.2008.
49. **Cluff T**, **Crevecoeur F**, **Scott SH.** Tradeoffs in optimal control capture patterns of human sensorimotor control and adaptation (Preprint). *bioRxiv* 730713, 2019. doi:10.1101/730713.
50. **Scott SH.** Optimal feedback control and the neural basis of volitional motor control. *Nat Rev Neurosci* 5: 532–546, 2004. doi:10.1038/nrn1427.
51. **Gribble PL**, **Ostry DJ.** Compensation for interaction torques during single- and multijoint limb movement. *J Neurophysiol* 82: 2310–2326, 1999. doi:10.1152/jn.1999.82.5.2310.

52. **Hollerbach MJ**, **Flash T.** Dynamic interactions between limb segments during planar arm movement. *Biol Cybern* 44: 67–77, 1982. doi:10.1007/BF00353957.
53. **Kurtzer I**, **Pruszynski JA**, **Scott SH.** Long-latency and voluntary responses to an arm displacement can be rapidly attenuated by perturbation offset. *J Neurophysiol* 103: 3195–3204, 2010. doi:10.1152/jn.01139.2009.
54. **Pruszynski JA**, **Kurtzer I**, **Scott SH.** The long-latency reflex is composed of at least two functionally independent processes. *J Neurophysiol* 106: 449–459, 2011. doi:10.1152/jn.01052.2010.
55. **Stein RB**, **Hunter IW**, **Lafontaine SR**, **Jones LA.** Analysis of short-latency reflexes in human elbow flexor muscles. *J Neurophysiol* 73: 1900–1911, 1995. doi:10.1152/jn.1995.73.5.1900.
56. **Cohen J.** *Statistical Power Analysis for the Behavioral Sciences* (2nd ed.). Hillsdale, NJ: Lawrence Erlbaum Associates, 1988.
57. **Crevecoeur F**, **Kurtzer I**, **Scott SH.** Fast corrective responses are evoked by perturbations approaching the natural variability of posture and movement tasks. *J Neurophysiol* 107: 2821–2832, 2012. doi:10.1152/jn.00849.2011.
58. **Hogan N.** The mechanics of multi-joint posture and movement control. *Biol Cybern* 52: 315–331, 1985. doi:10.1007/BF00355754.
59. **Besomi M**, **Hodges PW**, **Clancy EA**, **Van Dieën J**, **Hug F**, **Lowery M**, **Merletti R**, **Søgaard K**, **Wrigley T**, **Besier T**, **Carson RG**, **Disselhorst-Klug C**, **Enoka RM**, **Falla D**, **Farina D**, **Gandevia S**, **Holobar A**, **Kiernan MC**, **McGill K**, **Perreault E**, **Rothwell JC**, **Tucker K.** Consensus for experimental design in electromyography (CEDE) project: amplitude normalization matrix. *J Electromyogr Kinesiol* 53: 102438, 2020. doi:10.1016/j.jelekin.2020.102438.
60. **Lee RG**, **Tatton WG.** Long latency reflexes to imposed displacements of the human wrist: Dependence on duration of movement. *Exp Brain Res* 45: 207–216, 1982. doi:10.1007/BF00235780.
61. **Mutha PK**, **Sainburg RL.** Shared bimanual tasks elicit bimanual reflexes during movement. *J Neurophysiol* 102: 3142–3155, 2009. doi:10.1152/jn.91335.2008.
62. **Dimitriou M**, **Franklin DW**, **Wolpert DM.** Task-dependent coordination of rapid bimanual motor responses. *J Neurophysiol* 107: 890–901, 2012. doi:10.1152/jn.00787.2011.
63. **Omrani M**, **Diedrichsen J**, **Scott SH.** Rapid feedback corrections during a bimanual postural task. *J Neurophysiol* 109: 147–161, 2013. doi:10.1152/jn.00669.2011.
64. **Aimonetti JM**, **Morin D**, **Schmied A**, **Vedel JP**, **Pagni S.** Proprioceptive control of wrist extensor motor units in humans: dependence on handedness. *Somatosens Mot Res* 16: 11–29, 1999. doi:10.1080/08990229970618.
65. **Forgaard CJ**, **Franks IM**, **Maslovat D**, **Chua R.** Perturbation predictability can influence the long-latency stretch response. *PLoS One* 11: e0163854, 2016. doi:10.1371/journal.pone.0163854.
66. **Rothwell JC**, **Day BL**, **Berardelli A**, **Marsden CD.** Habituation and conditioning of the human long latency stretch reflex. *Exp Brain Res* 63: 197–204, 1986. doi:10.1007/BF00235664.
67. **Scott SH.** A functional taxonomy of bottom-up sensory feedback processing for motor actions. *Trends Neurosci* 39: 512–526, 2016. doi:10.1016/j.tins.2016.06.001.
68. **Pruszynski JA**, **Scott SH.** Optimal feedback control and the long-latency stretch response. *Exp Brain Res* 218: 341–359, 2012. doi:10.1007/s00221-012-3041-8.
69. **Nashed JY**, **Crevecoeur F**, **Scott SH.** Influence of the behavioral goal and environmental obstacles on rapid feedback responses. *J Neurophysiol* 108: 999–1009, 2012. doi:10.1152/jn.01089.2011.
70. **Nashed JY**, **Crevecoeur F**, **Scott SH.** Rapid online selection between multiple motor plans. *J Neurosci* 34: 1769–1780, 2014. doi:10.1523/JNEUROSCI.3063-13.2014.
71. **Diedrichsen J.** Optimal task-dependent changes of bimanual feedback control and adaptation. *Curr Biol* 17: 1675–1679, 2007. doi:10.1016/j.cub.2007.08.051.
72. **Diedrichsen J**, **Dowling N.** Bimanual coordination as task-dependent linear control policies. *Hum Mov Sci* 28: 334–347, 2009. doi:10.1016/j.humov.2008.10.003.
73. **Evarts EV**, **Tanji J.** Reflex and intended responses in motor cortex pyramidal tract neurons of monkey. *J Neurophysiol* 39: 1069–1080, 1976. doi:10.1152/jn.1976.39.5.1069.
74. **Cheney PD**, **Fetz EE.** Corticomotoneuronal cells contribute to long-latency stretch reflexes in the rhesus monkey. *J Physiol* 349: 249–272, 1984. doi:10.1113/jphysiol.1984.sp015155.
75. **Pruszynski JA**, **Omrani M**, **Scott SH.** Goal-dependent modulation of fast feedback responses in primary motor cortex. *J Neurosci* 34: 4608–4617, 2014. doi:10.1523/JNEUROSCI.4520-13.2014.
76. **Pruszynski JA**, **Kurtzer I**, **Nashed JY**, **Omrani M**, **Brouwer B**, **Scott SH.** Primary motor cortex underlies multi-joint integration for fast feedback control. *Nature* 478: 387–390, 2011. doi:10.1038/nature10436.
77. **Strick PL.** The influence of motor preparation on the response of cerebellar neurons to limb displacements. *J Neurosci* 3: 2007–2020, 1983. doi:10.1523/JNEUROSCI.03-10-02007.1983.
78. **Fromm C**, **Evarts EV.** Pyramidal tract neurons in somatosensory cortex: central and peripheral inputs during voluntary movement. *Brain Res* 238: 186–191, 1982. doi:10.1016/0006-8993(82)90781-8.
79. **Omrani M**, **Murnaghan CD**, **Pruszynski JA**, **Scott SH.** Distributed task-specific processing of somatosensory feedback for voluntary motor control. *Elife* 5: 1–17, 2016. doi:10.7554/eLife.13141.
80. **Norman RW**, **Komi PV.** Electromechanical delay in skeletal muscle under normal movement conditions. *Acta Physiol Scand* 106: 241–248, 1979. doi:10.1111/j.1748-1716.1979.tb06394.x.
81. **Cavanagh PR**, **Komi PV.** Electromechanical delay in human skeletal muscle under concentric and eccentric contractions. *Eur J Appl Physiol Occup Physiol* 42: 159–163, 1979. doi:10.1007/BF00431022.
82. **Saliba CM**, **Rainbow MJ**, **Selbie WS**, **Deluzio KJ**, **Scott SH.** Co-contraction uses dual control of agonist-antagonist muscles to improve motor performance (Preprint). *bioRxiv* 2020.03.16.993527, 2020. doi:10.1101/2020.03.16.993527.
83. **Taaffe DR**, **Lewis B**, **Marcus R.** Quantifying the effect of hand preference on upper limb bone mineral and soft tissue composition in young and elderly women by dual-energy X-ray absorptiometry. *Clin Physiol* 14: 393–404, 1994. doi:10.1111/j.1475-097X.1994.tb00398.x.
84. **Dare SS**, **Masilili G**, **Mugagga K**, **Ekanem PE.** Evaluation of bilateral asymmetry in the humerus of human skeletal specimen. *Biomed Res Int* 2019: 3194912, 2019. doi:10.1155/2019/3194912.
85. **Gutnik B**, **Skurvydas A**, **Zuoza A**, **Zuoziene I**, **Mickevičienė D**, **Alekrinskis A**, **Nash D.** Evaluation of bilateral asymmetry between upper limb masses in right-handed young adults of both sexes. *Percept Mot Skills* 120: 804–815, 2015. doi:10.2466/25.10.PMS.120v16x3.
86. **Sergi G**, **Perissinotto E**, **Zucchetto M**, **Enzi G**, **Manzato E**, **Giannini S**, **Bassetto F**, **Inelmen EM**, **Baldo G**, **Rinaldi G**, **Coin A.** Upper limb bone mineral density and body composition measured by peripheral quantitative computed tomography in right-handed adults: he role of the dominance effect. *J Endocrinol Invest* 32: 298–302, 2009. doi:10.1007/BF03345715.
87. **Winter DA.** *Biomechanics and Motor Control of Human Movement* (4th ed.). Hoboken, NJ: John Wiley and Sons Inc., 2009.
88. **Kurtzer I**, **Herter TM**, **Scott SH.** Random change in cortical load representation suggests distinct control of posture and movement. *Nat Neurosci* 8: 498–504, 2005. doi:10.1038/nn1420.
89. **Yadav V**, **Sainburg RL.** Handedness can be explained by a serial hybrid control scheme. *Neuroscience* 278: 385–396, 2014. doi:10.1016/j.neuroscience.2014.08.026.
90. **Yadav V**, **Sainburg RL.** Motor lateralization is characterized by a serial hybrid control scheme. *Neuroscience* 196: 153–167, 2011. doi:10.1016/j.neuroscience.2011.08.039.
91. **Scheidt RA**, **Ghez C.** Separate adaptive mechanisms for controlling trajectory and final position in reaching. *J Neurophysiol* 98: 3600–3613, 2007. doi:10.1152/jn.00121.2007.
92. **Ghez C**, **Scheidt R**, **Heijink H.** Different learned coordinate frames for planning trajectories and final positions in reaching. *J Neurophysiol* 98: 3614–3626, 2007. doi:10.1152/jn.00652.2007.
93. **Reuter EM**, **Cunnington R**, **Mattingley JB**, **Riek S**, **Carroll TJ.** Feedforward compensation for novel dynamics depends on force field orientation but is similar for the left and right arms. *J Neurophysiol* 116: 2260–2271, 2016. doi:10.1152/jn.00425.2016.
94. **Stockinger C**, **Thürer B**, **Focke A**, **Stein T.** Intermanual transfer characteristics of dynamic learning: direction, coordinate frame, and consolidation of interlimb generalization. *J Neurophysiol* 114: 3166–3176, 2015. doi:10.1152/jn.00727.2015.